



Recyclable Zr/Hf-Containing Acid-Base Bifunctional Catalysts for Hydrogen Transfer Upgrading of Biofuranics: A Review

Yixuan Liu^{1†}, Xixi Liu^{2†}, Mingrui Li¹, Ye Meng¹, Jie Li¹, Zehui Zhang² and Heng Zhang^{1*}

¹State Key Laboratory Breeding Base of Green Pesticide and Agricultural Bioengineering, Key Laboratory of Green Pesticide and Agricultural Bioengineering, Ministry of Education, State-Local Joint Laboratory for Comprehensive Utilization of Biomass, Center for Research and Development of Fine Chemicals, Guizhou University, Guiyang, China, ²Key Laboratory of Catalysis and Materials Sciences of the Ministry of Education, South-Central University for Nationalities, Wuhan, China

OPEN ACCESS

Edited by:

Yaqiong Su,
Xi'an Jiaotong University, China

Reviewed by:

Jian He,
Jishou University, China
Anping Wang,
Guizhou Normal University, China
Hu Pan,
Jiaxing University, China

*Correspondence:

Heng Zhang
hzhang23@gzu.edu.cn

[†]These authors have contributed
equally to this work

Specialty section:

This article was submitted to
Green and Sustainable Chemistry,
a section of the journal
Frontiers in Chemistry

Received: 10 November 2021

Accepted: 22 November 2021

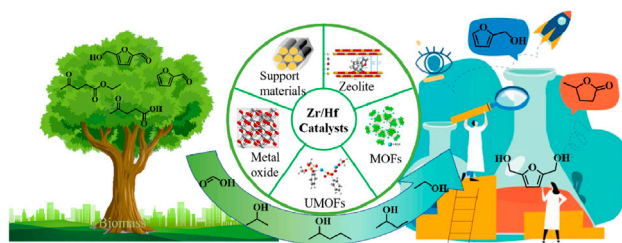
Published: 21 December 2021

Citation:

Liu Y, Liu X, Li M, Meng Y, Li J, Zhang Z
and Zhang H (2021) Recyclable Zr/Hf-
Containing Acid-Base Bifunctional
Catalysts for Hydrogen Transfer
Upgrading of Biofuranics: A Review.
Front. Chem. 9:812331.
doi: 10.3389/fchem.2021.812331

The massive burning of a large amount of fossil energy has caused a lot of serious environmental issues (e.g., air pollution and climate change), urging people to efficiently explore and valorize sustainable alternatives. Biomass is being deemed as the only organic carbon-containing renewable resource for the production of net-zero carbon emission fuels and fine chemicals. Regarding this, the selective transformation of high-oxygen biomass feedstocks by catalytic transfer hydrogenation (CTH) is a very promising strategy to realize the carbon cycle. Among them, the important Meerwein-Ponndorf-Verley (MPV) reaction is believed to be capable of replacing the traditional hydrogenation strategy which generally requires high-pressure H₂ and precious metals, aiming to upgrade biomass into downstream biochemical products and fuels. Employing bifunctional heterogeneous catalysts with both acidic and basic sites is needed to catalyze the MPV reaction, which is the key point for domino/cascade reaction in one pot that can eliminate the relevant complicated separation/purification step. Zirconium (Zr) and hafnium (Hf), belonging to transition metals, rich in reserves, can demonstrate similar catalytic efficiency for MPV reaction as that of precious metals. This review introduced the application of recyclable heterogeneous non-noble Zr/Hf-containing catalysts with acid-base bifunctionality for CTH reaction using the safe liquid hydrogen donor. The corresponding catalysts were classified into different types including Zr/Hf-containing metal oxides, supported materials, zeolites, metal-organic frameworks, metal-organic hybrids, and their respective pros and cons were compared and discussed comprehensively. Emphasis was placed on evaluating the bifunctionality of catalytic material and the key role of the active site corresponding to the structure of the catalyst in the MPV reaction. Finally, a concise summary and prospect were also provided centering on the development and suggestion of Zr/Hf-containing acid-base bifunctional catalysts for CTH.

Keywords: transfer hydrogenation, meerwein-ponndorf-verley reaction, Zr/Hf-containing catalyst, acid-base bifunctionality, biomass conversion



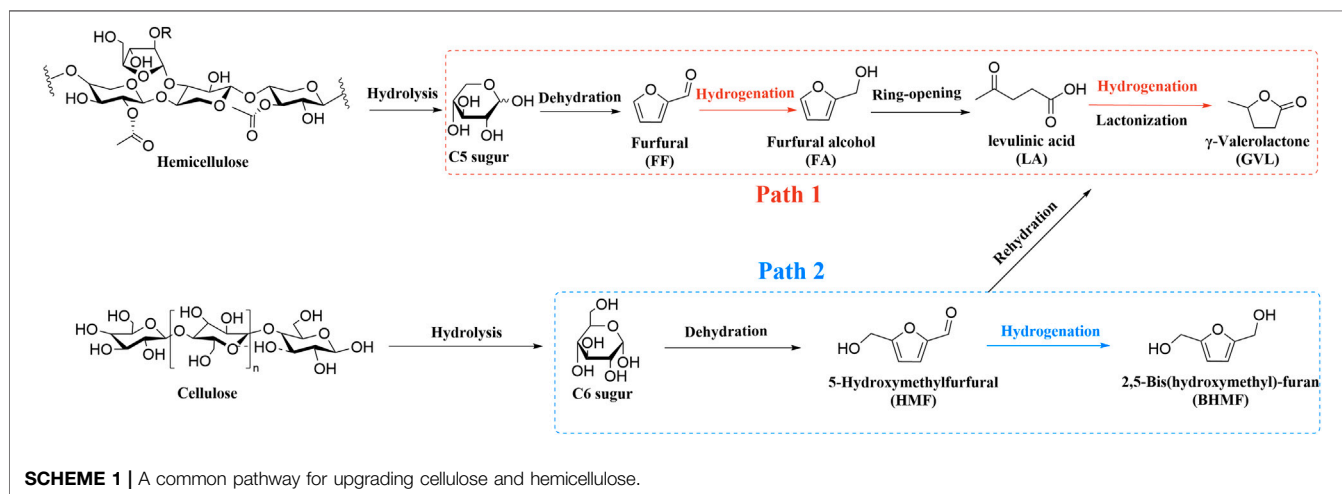
GRAPHIC ABSTRACT |

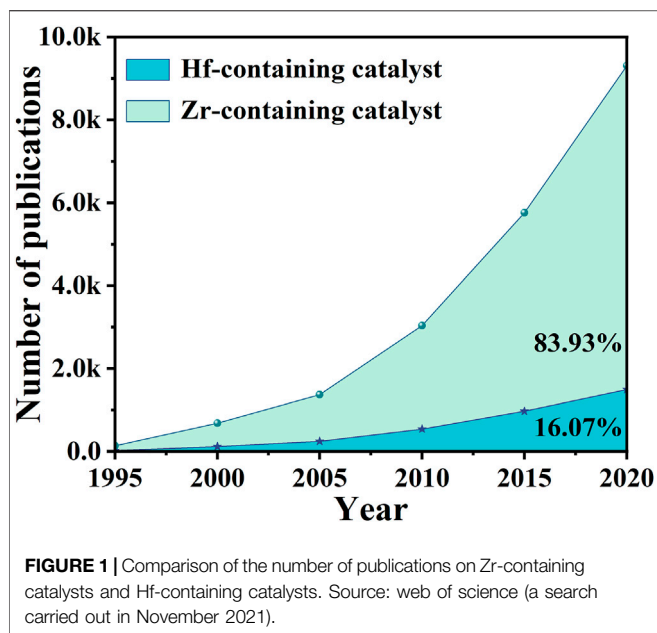
This review introduced the application of recyclable heterogeneous non-noble Zr/Hf-containing catalysts with acid-base bifunctionality for CTH reaction using the safe liquid hydrogen donor. The corresponding catalysts were classified into different types including Zr/Hf-containing metal oxides, supported materials, zeolites, metal organic frameworks, metal organic hybrids, and their respective pros and cons were compared and discussed comprehensively. Emphasis was placed on evaluating the bifunctionality of catalytic material and the key role of active site corresponding to the structure of the catalyst in the MPV reaction.

INTRODUCTION

The large-scale exploitation of fossil-based resources exists alongside environmental deterioration like global warming, acid rain, and air pollution (Tripathi et al., 2016; Valderrama Rios et al., 2018; Ahmad et al., 2019; Brauer et al., 2021; Schwarzman et al., 2021). On the eve of the “26th United Nations Climate Change Conference” in 2021, more than 230 major journals around the world jointly published an editorial to warn global leaders to act immediately for climate change (Atwoli et al., 2021). These serious problems compel humans to seek renewable and clean resources for the sustainable supply of fuels and chemicals (Zhang et al., 2020; Khan et al., 2021; Osman et al., 2021; Rode et al., 2021; Wu et al., 2021; Yu et al.,

2021; Zantye et al., 2021; Zhang et al., 2021a). Biomass acts as the only organic carbon-containing source on earth that mainly contains carbon, hydrogen, and oxygen species (Wang et al., 2014b; Han et al., 2019; Spinelli et al., 2019; Zhu et al., 2019; Pattnaik et al., 2021). Biomass energy is ubiquitous, rich, renewable, and sustainable and its main sources are firewood, wood waste, agricultural straw, livestock manure, sugar crop waste, municipal waste with sewage, and aquatic plants, respectively (Li et al., 2018a; Luo et al., 2019; Abomohra et al., 2020; Sudarsanam et al., 2020; Wu et al., 2020). Compared with other renewable energy sources, it has unique advantages in terms of the reuse of waste resources and the production of fuels and high-value chemicals. It is highly valued in many aspects such as scientific research, politics, and the economy (Wu et al., 2018a; Mathimani and Mallick, 2019; Welch et al., 2021; Tan et al., 2022). There is a significant long-term two-way causal relationship between biomass energy consumption and economic growth (Ajmi and Inglesi-Lotz, 2020; Sabyrzhay et al., 2021). Hence, biomass has broad application potential in the future production and life of mankind (Kumar et al., 2015; Gawade et al., 2016; Hu et al., 2017; Liu et al., 2021c). However, compared to the desired products especially for fuels or fuel additives, biomass-derived feedstocks generally possess higher oxygen content (Prasomsri et al., 2013; Liao et al., 2014; Li et al., 2020a; Li et al., 2020b; Wang et al., 2020a). It is still necessary to further process the biomass feedstock to upgrade its functional groups (Dabros et al., 2018; Li et al., 2019b; Iglesias et al., 2020





Tan et al., 2021). In the field of biomass upgrading, the most widely used approach is to convert biomass (e.g., cellulose and hemicellulose) into a series of furan compounds *via* cascade reactions (**Scheme 1**) (Zhou and Zhang, 2016; Liu et al., 2019; Chen et al., 2021b). Among furan compounds, γ -valerolactone (GVL) is recognized as a kind of versatile chemical building block (Liu et al., 2021a; Kerkel et al., 2021; Delgado et al., 2022). It's a green organic solvent and can also be used as a precursor for the manufacture of liquid fuels (Huang et al., 2018; Crabtree, 2019). 5-Hydroxymethylfurfural (HMF) has various furan rings coupled with the hydroxyl and aldehyde groups present at the exocyclic carbon atoms (Chen et al., 2018; Zhang et al., 2021b; Sarkar et al., 2021). It can be converted to levulinic acid (LA) and further produced GVL, or it can be converted to 2,5-bis(hydroxymethyl)furan (BHMF) through another route. (Kou et al., 2016; Prielcel et al., 2018; Li and Jiang, 2019). Therefore, the main conversion path of this article is the production of furan compounds such as GVL and BHMF.

Many reactions are involved in these processes, such as dehydration, hydrogenation, ring-opening (Yang et al., 2017b; Iriondo et al., 2017; Solanki and Rode, 2019). But the key speed-determining step is transfer hydrogenation via the Meerwein-Ponndorf-Verley (MPV) reduction reaction, which is also called indirect catalytic transfer hydrogenation (CTH) (Singh et al., 2015; Li et al., 2018c; Shao et al., 2021). Different kinds of alcohols can be used as H-donors in relatively mild conditions, achieving efficient catalysis performance for CTH reaction of the carbonyl group of α , β -unsaturated aldehyde/ketone (Mondelli et al., 2020). Therefore, the C=O bond is hydrogenated while retaining the C=C bond (Wu et al., 2018b; Li et al., 2018d; Jin et al., 2019; Liu et al., 2021d). Heterogeneous catalysts were widely used in MPV reduction reactions, which can be easily recycled and also can effectively reduce industrial production costs (Santana and Krische, 2021; Pan et al., 2022). It goes without saying that the choice of materials is of great importance for the

relevant catalytic system. In contrast to the indirect hydrogenation via MPV reaction using alcohol as a hydrogen donor (H-donor), there is another direct hydrogenation reaction in CTH that uses precious metals and H₂. Although precious metals (e.g., Ru, Pd, Ir, Pt) were widely studied for direct CTH, the prices were not suitable for industrialization (Tuteja et al., 2014; Brethauer and Studer, 2015; Cao et al., 2017; Wang T. et al., 2020). On the other hand, non-noble metals (e.g., Fe, Co, Cu, Ni) were restricted because of relatively low activity and/or product selectivity (Hu et al., 2019a; Zhang et al., 2019b; Shi et al., 2019; Jiang et al., 2020). These disadvantages have prompted scientists to explore alternative catalysts, which can balance economy and high selectivity (Yin and Shen, 2020). Thus, researchers discovered that transition metal carbides have similar properties with Pt metal (Pang et al., 2019). Since transition metals have both metallic and acidic properties, they can be used as effective catalysts for the upgrading of oxygen-containing compounds derived from biomass (Choi et al., 2011; Heard et al., 2016; Gonell et al., 2017; Wagner et al., 2021). It has good corrosion resistance and is not easily corroded by general acid-base aqueous solutions (Sullivan et al., 2016; Wei et al., 2021). Among the transition metals, Zr and Hf metals with similar properties have set off a wave of research craze in the field of CTH (Champness, 2011; Li et al., 2016a; B et al., 2018). **Figure 1** shows that from 1995 to 2021, the number of articles published on Zr-based catalysts in 2020 is even 5 times than that of Hf-based catalysts. Although the metals of the fourth subgroup have similar properties, the research of Hf-based catalysts in this field is far from enough, which is also a trend and direction of future exploration.

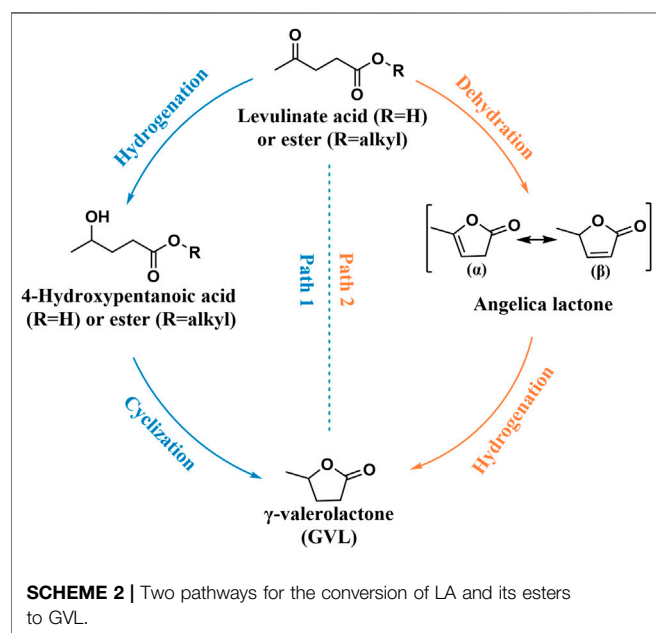
There are some relevant reviews about biomass conversion and CTH reaction. For example, a comprehensive review of bifunctional catalysts to convert biomass into biofuels was proposed by Li et al. (2016a). What's more, some reviews focused on the production of GVL from lignocellulosic biomass, (Tang et al., 2014b; Ye et al., 2020) and other studies paid attention to the mechanism and interface effects of heterogeneous CTH (Gilkey and Xu, 2016; Liu et al., 2021b). However, as far as we know, there is no review of the application of transition metal Zr/Hf catalysts used for the synthesis of biofurans compounds. In this review, the target is to selectively discuss the latest developments of various types of Zr/Hf-containing catalysts through MPV reduction to upgrade biomass-derived feedstocks. It will focus on exploring the specific mechanism of the catalysts' active site (Lewis/Brønsted acid and base) in each biomass upgrading reaction. Finally, some opportunities and challenges faced by CTH for efficiently converting biomass into fuels or high-value chemicals have also been prospected appropriately.

ZR/HF-CONTAINING METAL OXIDE CATALYSTS

Zr has excellent high-temperature resistance, and its melting point is as high as 2,700°C. Even if it is heated to 1900°C, it will still not react with molten Al, Fe, Ni, Pt, and other metals.

TABLE 1 | Zr/Hf-based metal oxide catalysts.

Entry	Substrate	Catalyst	Condition	H-donor	Product	Conv. (%)	Yield (%)	References
1	LA/FA	Ag-Ni/ZrO ₂	220°C, 5 h	Water	GVL	100	99	Hengne et al. (2014)
2	LA	HCl/ZrO(OH) ₂	240°C, 2 h	2-BuOH	GVL	99.9	92.4	Tang et al. (2015)
3	LA	Cu-ZrO ₂	200°C, 5 h	Water	GVL	100	99.9	Hengne and Rode, (2012)
4	ML	Cu-ZrO ₂	200°C, 5 h	Methanol	GVL	95	92	Hengne and Rode, (2012)
5	ML	Ni/ZrO ₂	90°C, 20 h	2-PrOH	GVL	100	92	Sakakibara et al. (2019)
6	ML	Cu/ZrOCO ₃	180°C, 7 h	2-PrOH	GVL	99	89.79	Ma et al. (2020)
7	EL	ZrO(OH) ₂ ·xH ₂ O	240°C, 1 h	EtOH	GVL	89.1	75.3	Tang et al. (2014a)
8	EL	ZrO ₂ -B ₂ O ₃	200°C, 4 h	2-PrOH	GVL	95.1	88.5	He et al. (2016a)
9	EL	ZrO ₂	250°C, 3 h	EtOH	GVL	95.5	81.5	Tang et al. (2013)
10	EL	Al ₇ Zr ₃ -300	220°C, 4 h	2-PrOH	GVL	95.5	83.2	He et al. (2016b)
11	EL	ZrFeO _x	270°C, 3 h	EtOH	GVL	94.2	87.2	Li et al. (2015)
12	EL	Zr ₃ Ni ₅	200°C, 3 h	2-PrOH	GVL	97.2	95.2	Li et al. (2016b)
13	EL	Ti/Zr	180°C, 6 h	2-PrOH	GVL	100	90.1	Yang T. et al. (2017)
14	BL	ZrO ₂	150°C, 16 h	2-BuOH	GVL	99.9	84.7	Chia and Dumesic (2011)
15	FF	Zr(OH) ₄ @CoFe ₂ O ₄	160°C, 4 h	2-PrOH	FA	95.4	92.6	Hou et al. (2021)
16	FF	HfO(OH) ₂ ·xH ₂ O	180°C, 8 h	2-PrOH	GVL	100	64.2	Li M. et al. (2021)
17	HMF	ZrO(OH) ₂	150°C, 2.5 h	EtOH	BHMF	94.1	88.9	Hao et al. (2016)



Commercial zirconium oxide (ZrO₂) has been used in the nuclear energy industry, national defense industry, electronic components, ceramic carbon powder, along with high-temperature resistant materials, etc. (Ishikawa et al., 2017). Among them, ZrO₂ was also used in the field of catalysis due to its excellent chemical stability and high surface chemical activity (Liu et al., 2002; Zhu et al., 2004; Gonell et al., 2017). As a typical weak acid-base bifunctional material, ZrO₂ and HfO₂ have exceptional catalytic performance in CTH reaction (Paniagua et al., 2021). In Zr/Hf-containing metal oxide catalysts, as shown in **Table 1**, the main researches in recent years are classified and summarized according to the reaction substrate.

LA and its Esters as Substrates

LA as a Substrate

LA was listed as one of the 12 high-value chemicals from biomass by the U.S. DE (Bogale et al., 2019). It was considered as a significant platform compound for the synthesis of organic chemicals (Hu et al., 2021; Tian et al., 2021). In general, there are usually two reaction pathways of heterogeneous catalysis in the production of GVL using LA and its esters [e.g., methyl levulinate (ML), ethyl levulinate (EL), butyl levulinate (BL)] as substrates. These two reaction pathways mainly depend on the controlled reaction conditions and the catalyst used during the reaction (**Scheme 2**) (Dutta et al., 2019). In path 1, hydrogenation reaction is prone to occur at lower temperatures to promote the conversion of LA to 4-hydroxypentanoic acid under the water phase system, which is then dehydrated to GVL under the action of a catalyst. In path 2, LA is first dehydrated to form angelica lactone at higher temperatures, which is then hydrogenated to obtain GVL. In short, hydrogen and dehydration can occur either way. But under different control reaction conditions, the sequence of these two processes will change, accordingly.

Ag-Ni/ZrO₂ catalyst has attracted researchers' attention due to its magnetic properties that are easy to separate (Hengne et al., 2014). The two metals play a synergistic effect in the transformation of LA and furfuryl alcohol (FA) (1:1) mixture to GVL. It also proved that Ag-Ni/ZrO₂ has a comprehensive scope of applications in the one-pot CTH of biomass-derived C3 to C6 molecules, with relatively high conversion and selectivity (>80%) (entry 1 of **Table 1**). In addition to using high-purity synthetic chemicals as substrates, researchers were further required to explore some methods that can be closer to biomass raw materials to produce GVL. Tang et al. developed an *in-situ* catalyst generation system to produce GVL (Tang et al., 2015). The system can decompose the HCl/ZrO(OH)₂ catalyst in LA and 2-butanol (2-BuOH) solution autonomously and then a 2-BuOH *in-situ* H-donor was employed to catalyze the cyclization of LA esterification to GVL. The highlight of this

system was that crude LA can be directly used to produce GVL. The crude LA was extracted from the acid hydrolysis of cellulose (47.8% yield), and flowed into 2-BuOH. Finally, 2-BuOH was used to extract LA and FA from the cellulose hydrolysate (90.2% v. s. 15.1%), as depicted in entry 2 of **Table 1**. Even in the presence of humin after use, a GVL yield of 82.0% can be successfully obtained. In addition, when investigating the influence of solvent, it was found that the GVL yield of 2-BuOH was much lower than that of 2-Propanol (2-PrOH) (27.5% vs. 62%) at 200°C because the steric effect of 2-BuOH was stronger than 2-PrOH. Continue to increase the temperature to 240°C, the steric effect of 2-BuOH can be overcome, and the yield can be increased to 84.5%. According to Derjaguin–Landau–Verwey–Overbeek (DLVO) theory, the principle of the catalysts agglomeration phenomenon was speculated. That was, the adsorbed LA and H-donors enhanced the electrostatic repulsion between the $\text{ZrO}(\text{OH})_2$ particles formed *in situ*, thereby preventing further agglomeration in 2-BuOH. In other words, the dispersibility and morphology of $\text{ZrO}(\text{OH})_2$ particles that played a key catalytic role mainly depended on the solvent and the substrate. Most Cu-ZrO₂ catalysts were prepared by co-precipitation with mixed precursors (entry 3 of **Table 1**) (Hengne and Rode, 2012). Its excellent catalytic performance should be attributed to its strong surface acidity. The effective active component in the catalytic hydrogenation process was the reduced Cu particles dispersed on the catalyst surface. The introduction of Cu into the tetragonal ZrO₂ lattice can enhance the adhesion of these particles as well as make them dispersed. It can also enhance the number of acid sites, among which Lewis acid was also determined to enhance the transfer hydrogenation activity. Changing the starting material from LA to ML and the H-donor from water to methanol, Cu-ZrO₂ still had a very objective activity (entry 4 of **Table 1**).

ML as a Substrate

Ni/ZrO₂ was also used to convert ML and LA to GVL, which were catalyzed and reacted to test the active materials (Sakakibara et al., 2019). It was concluded that the Ni contributed to the hydrogenation of ML and LA, and the Zr contributed to the lactonization of the hydrogenated product. Under relatively mild conditions of 90°C, the GVL yield reached 92% (entry 5 of **Table 1**). But the disadvantage was that the reaction time was as long as 20 h. It is well known that GVL can be directly hydrogen transfer catalyzed by ZrOCO₃. Further studies by Ma et al. found that using ZrOCO₃ as a carrier, the introduction of Cu/Cu⁺ can increase the CTH activity (entry 6 of **Table 1**) (Ma et al., 2020). And Cu/ZrOCO₃ can also further convert GVL into 1,4-Pentanediol (1,4-PDO) through the MPV reaction. This may be caused by the coordination effect between the Cu and the acid-base sites of the carrier. Cu vacancy (Cu⁰) and Cu ion (Cu⁺) were formed after *in-situ* reduction. Cu⁺ can be used as Lewis acid to adsorb and activate the C=O group through the electron lone oxygen atom pair. Alcohol can be excited to become an activated metal hydride on the Cu⁰ surface, and then attack the activated C=O group to form an O-H group. ZrOCO₃ was an amphoteric catalyst, which can also promote the MPV reaction through six-membered ring intermediates. In

addition, amphoteric carriers (such as $\text{Al}(\text{OH})_3$ and ZrOCO_3) contained more acid-base sites than basic carriers (such as $\text{Mg}_2(\text{OH})_2\text{CO}_3$ and ferric hydroxide), demonstrating a better catalytic activity accordingly.

EL as a Substrate

EL was used to prepare GVL through CTH. Tang et al. used $\text{ZrO}(\text{OH})_2 \cdot x\text{H}_2\text{O}$ catalyst to obtain 89.1% EL conversion and 75.3% GVL yield in ethanol (EtOH) under 240°C for 1 h (entry 7 of **Table 1**) (Tang et al., 2014a). First, EtOH was adsorbed on the surface of the catalyst and dissociated into the corresponding alkoxide. EL obtained two hydrogen atoms from EtOH to obtain the intermediate ethyl 4-hydroxypentanoate (4-HPE). Then 4-HPE underwent intramolecular transesterification to obtain the final product GVL. But there was another reaction path, 4-HPE and EtOH were etherified to produce by-product 4-ethoxypentanoate (4-EPE). Self-aldol condensation may occur between EL, GVL, and aldehyde dehydrogenated from EtOH, and the formation of trace by-products can be ignored in the system. Doping boric acid in Zr-containing catalysts can increase its acid content, but the traditional wet impregnation method was difficult to control the leaching of the boron component during the reaction. Therefore, He et al. used the sol-gel method to improve the synthesis of the mesoporous Zr/boron mixed oxides catalyst (He et al., 2016a). $\text{ZrOCl}_2 \cdot 8\text{H}_2\text{O}$ and boric acid were stirred at 40°C for 3 h and then transferred to an oven to evaporate the solvent for 4 h after sonication. After drying at 80°C for 1 day, it was calcined at 450°C for 6 h. In general, the preparation process was relatively simple. With this amorphous material catalyst, 95.1% EL conversion and 88.5% GVL yield were obtained at 200°C for 4 h (entry 8 of **Table 1**). As the boron content increased, the surface area, acid density, and alkali density of the mesoporous material improved correspondingly. Nonetheless, adding too much boron to ZrO₂ will reduce the alkali density and inhibit the alkalinity of the catalyst. However, ZrO₂ catalyst still existed the disadvantage of high temperature or long time during the reaction (entry 9 of **Table 1**) (Tang et al., 2013). To address this issue, Al-Zr mixed metal catalysts were prepared by the co-precipitation method (He et al., 2016b). $\text{ZrOCl}_2 \cdot 8\text{H}_2\text{O}$ and $\text{Al}(\text{NO}_3)_3 \cdot 9\text{H}_2\text{O}$ were dissolved in deionized water, and then an aqueous ammonia solution (25–28%) was added dropwise. Next, the solution underwent a series of methods such as pH adjustment, aging, drying, and calcination to obtain the target solid catalyst. It was found that when Al was added to ZrO₂, the surface area was enlarged and the number of effective acid and base sites of the catalyst was increased. With 2-PrOH as the H-donor and solvent, the EL conversion was 95.5% and the GVL yield was 83.2% at 220°C (entry 11 of **Table 1**). Both formic acid and LA can be obtained from sugars in an equimolar ratio were found by Li et al. Therefore, if FA is used as an H-donor and LA is used as a substrate to synthesize GVL, it is obviously a reasonable system. Nano-FeZrO_x materials have also been reported to have magnetic recyclable properties. The acid-base bifunctional catalysts of superparamagnetism were synthesized through the reaction of

solvent heat treatment and hydrolysis condensation. Upon using EtOH as H-donor, effective conversion of EL to GVL was successfully conducted. A series of FeZrO_x catalysts with different Fe-Zr ratios were prepared (entry 11 of **Table 1**) (Li et al., 2015). It was found that ZrFeO (1:3)-300 with Fe_3O_4 covered by a ZrO_2 layer had an appropriate distribution of acid-base sites as well as a medium surface area and pore size. The yield of GVL can be reached as high as 87.2% (3 h, 230°C). In addition, the catalyst containing Zr and Fe can also be combined with the solid acid HY2.6 to directly convert sugar into GVL, with a yield of 44.7%. To be specific, $\text{Ni}(\text{NO}_3)_2 \cdot 6\text{H}_2\text{O}$ and $\text{ZrOCl}_2 \cdot 8\text{H}_2\text{O}$ were used to synthesize magnetic Ni-Zr nanocatalysts for the conversion of various biomass derivatives (Li et al., 2016b). This hydrogen-reduced magnetic Zr_5Ni_5 nanoparticles (<20 nm) catalyzed EL to produce GVL (95.2% yield) within 3 h at 200°C (entry 12 in **Table 1**). Surprisingly, the system can also catalyze the conversion of fructose, glucose, cellobiose, and carboxymethyl cellulose into GVL and EL in one pot, with a total yield of 69.5, 60.1, 56.0, and 51.5%, respectively. And ICP-OES detected that only 0.3 wt% Ni and 0.5% Zr were immersed in 2-PrOH. The very small amount of immersion can clearly explain the heterogeneity of the catalyst and the nature of easy recycling. In addition, the nano-catalyst was combined with the solid acid HY6, the catalyst was easily attracted by the permanent magnet because of its magnetic properties. The used catalyst was washed 3 times with EtOH and dried, and it can be reused more than 5 times. In addition, the catalyst can be recovered by more than 89–93%, which is very suitable from an economic and convenient point of view.

Also using EL as a substrate, Yang et al. developed a microsphere Ti/Zr porous oxide catalyst through a sol-gel process combined with solvent heat treatment (Yang et al., 2017a). With hexadecyl amine (HDA) as the directing agent, the catalysts (Ti_xZr_y) with different Ti/Zr molar ratios that have $-\text{Zr}-\text{O}-\text{O}-\text{Zr}-$ network were developed. This not only allowed the mixed oxide to have adjustable porosity and large surface area but also enhanced its acidity and alkalinity. Compared to the amorphous structure of commercial titanium oxide (TiO_2) and ZrO_2 , Ti/Zr oxides were spherical. Experiments and tests showed that Ti_2Zr_8 had the largest surface area (385 m^2/g), appropriate acidity (1.12 mmol/g), and alkalinity (0.46 mmol/g), which was the best option. In general, if there was a base in the reaction system, the reaction activity will be improved. The increase in reactivity benefited from the ability to accept hydroxyl protons from the H-donor. There were also many sources of bases, which can be organic ligands, solvent molecules, or dissolved alkaline substances. The catalyst can be reused at least 6 times, and it can still obtain almost complete EL conversion and GVL yield of greater than 84.4% (entry 13 of **Table 1**). BL was also one of the common LA and its esters (entry 14 of **Table 1**) (Chia and Dumesic, 2011).

FF (Furfural) as a Substrate

For the conversion of FF to FA, the hollow core-shell magnetic catalyst named $\text{Zr}(\text{OH})_4@\text{CoFe}_2\text{O}_4$ was developed and employed for CTH (entry 15 of **Table 1**) (Hou et al., 2021). Firstly, 2-PrOH

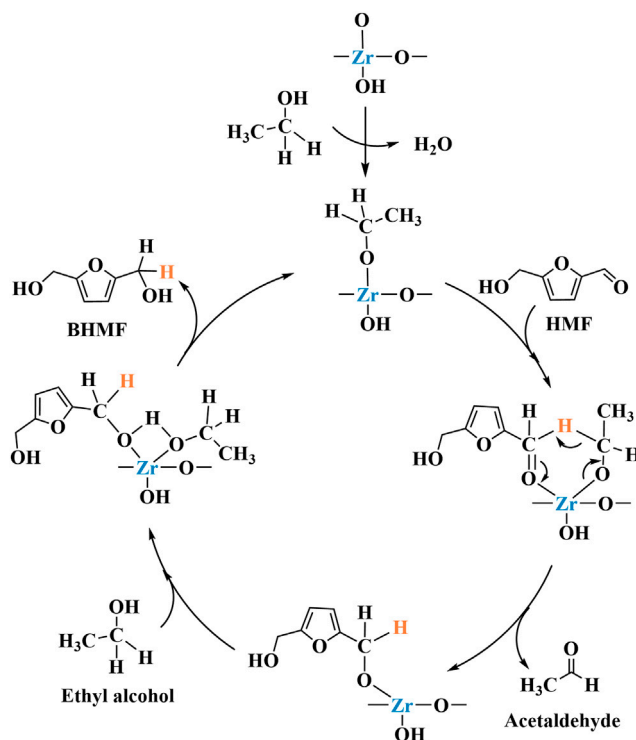
was adsorbed on the surface of $\text{Zr}(\text{OH})_4$ and interacted with Lewis acid sites (Zr^{4+}) and base sites (O^{2-}) to form metal alkoxide. Then, the O atom on the carbonyl group of FF was activated by Zr^{4+} . A typical six-membered ring transition state was formed. Then hydride transfer from alkoxide to the carbonyl group of FF was accomplished. Finally, the newly formed FA was desorbed from the surface of the catalyst along with acetone, and the active site of Zr^{4+} was re-exposed for the next run.

One-pot conversion of FF to GVL can use commercial HfCl_4 as a catalyst (Li et al., 2021b). With 2-PrOH as H-donor, the yield of GVL reached 65.5% in 8 h at 180°C (entry 16 of **Table 1**). During the reaction, HfCl_4 is hydrolyzed *in situ* to produce $\text{HfO}(\text{OH})_2 \cdot x\text{H}_2\text{O}$ (medium Lewis basic) and HCl (strong Brønsted acid). Together with the Lewis acid site (Hf^{4+}), they play a synergistic effect in the cascade reaction process, which is significantly improved the catalytic activity. HfCl_4 provides Lewis acid site (Hf^{4+}), while $\text{HfO}(\text{OH})_2 \cdot x\text{H}_2\text{O}$ and HCl were gradually *in situ* generated by the HfCl_4 hydrolysis in 2-PrOH due to the presence of residual water to provide Lewis base site (O^{2-}) and Brønsted acid site (HCl), respectively. 1) The carbonyl group of FF was adsorbed on the Lewis acid site (Hf^{4+}), and 2-PrOH with the oxygen and hydrogen atom of the hydroxyl group were respectively adsorbed to the Lewis acidic Hf^{4+} and the Lewis basic oxo-ion site. Then, a six-membered ring transition state was formed to complete the transfer hydrogenation process. FF was converted to Furfuryl Alcohol (FA), at the same time the 2-PrOH was transformed to acetone. 2) FA reacting with 2-PrOH was catalyzed by Lewis acid sites to form isopropyl furfuryl ether (FE) by etherification reaction. 3) The conversion of IPL to isopropyl 4-hydroxyvalerate (4-HPE) via transfer hydrogenation was similar to that of FF to FA, which was also catalyzed by the Lewis acid-base site ($\text{Hf}^{4+}-\text{O}^{2-}$). 4) 4-HPE undergone cyclization reaction to produce equivalent GVL was conducted in the presence of acid sites. In addition, the recycled catalysts can effectively catalyze the conversion of FF to FA after being calcined (2-PrOH as H-donor and the yield is 60.5% at 170°C for 1.5 h).

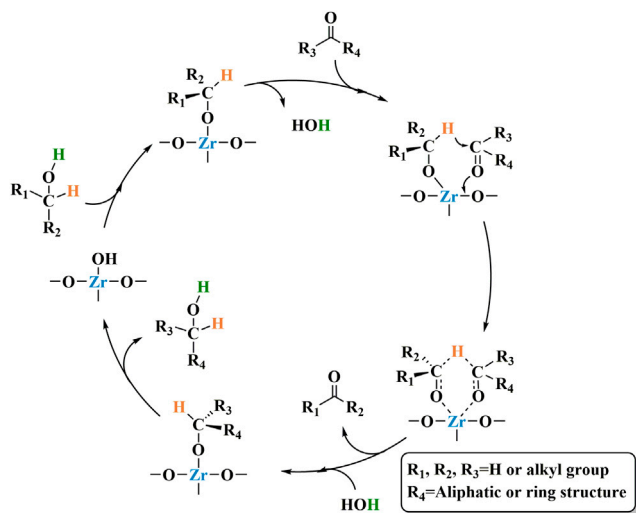
HMF as a Substrate

CTH mechanism of HMF on $\text{ZrO}(\text{OH})_2$ was shown in **Scheme 3** (Hao et al., 2016). The carbonyl oxygen of HMF coordinated with the alkoxide a to form a six-membered ring transition state b on Zr species. The hydride was transferred from the alkoxide to the carbonyl of HMF in b. Meanwhile, the new carbonyl (aldehyde) dissociated and released the intermediate c. Then another EtOH coordinated with it to form d. At the end, the newly reduced carbonyl (BHMF) dissociated to regenerate the alkoxide a. The BHMF yield of 88.9% can be achieved by reacting for 2.5 h at 150°C (entry 17 of **Table 1**).

The mechanism by which Zr-containing metal oxides catalyze the completion of transfer hydrogenation of carbonyl compounds via MPV reduction reaction is shown in **Scheme 4**. First, the alcohol is absorbed by the Lewis acid sites in the catalyst to form the corresponding alkoxide (Gonell et al., 2017). Then, the carbonyl group combines with the alkoxide to produce a six-membered ring transition state (Injongkol et al., 2017). Finally, a coordinated hydrogen transfer occurs



SCHEME 3 | The mechanism for the CTH of HMF into BHMf over ZrO(OH)₂ (Hao et al., 2016).



SCHEME 4 | General reaction mechanism of hydrated ZrO₂.

between the activated carbonyl compound and the alkoxide. process. At the same time, the obtained new carbonyl chemical substance ketone is released. Finally, another alcohol molecule participates in the reaction to generate the target product and the starting alkoxide.

ZR/HF-CONTAINING SUPPORTED MATERIAL CATALYSTS

The carrier material usually uses mesoporous molecular sieves, which generally have relatively large specific surface areas, large

TABLE 2 | Zr/Hf-containing supported material catalysts.

Entry	Substrate	Catalyst	Condition	H-donor	Product	Conv. (%)	Yield	References
1	LA	ZrO ₂ /SBA-15	150°C, 2 h	2-PrOH	GVL	99	83	Kuwahara et al. (2014)
2	ML	ZrO ₂ /SBA-15	150°C, 2 h	2-PrOH	GVL	98	88	Kuwahara et al. (2014)
3	ML	ZrO ₂ (10)/SBA-15	150°C, 3 h	2-PrOH	GVL	99.5	91	Kuwahara et al. (2017)
4	EL	ZrO ₂ /SBA-15	150°C, 2 h	2-PrOH	GVL	86	81	Kuwahara et al. (2014)
5	EL	Chitosan-Hf	160°C, 8 h	2-PrOH	GVL	100	97	Wang T. et al. (2020)
6	EL	Chitosan-Zr	160°C, 8 h	2-PrOH	GVL	100	97	Wang T. et al. (2020)
7	FF	ZrO ₂ -SBA-15	170°C, 7 h	2-PrOH	GVL	99	37	Iglesias et al. (2018)
8	FF	Fe ₃ O ₄ /ZrO ₂ @MCM-41	150°C, 24 h	2-PrOH	GVL	99.3	80.8	Gao et al. (2021)
9	FF	TPA-ZrO ₂ -SBA-15	170°C, 11 h	2-PrOH	GVL	100	81	Srinivasa Rao et al. (2021)
10	FF	Zr-SBA-15	110°C, 6 h	2-PrOH	FA	63	40	Iglesias et al. (2015)

pore sizes, along with regular pore structures (Taniya et al., 2010). Mesoporous molecular sieves are regarded as good shape-selective catalysts and have better catalytic activity and selectivity than zeolite molecular sieves when organic macromolecular substances participate (Shen et al., 2014). In addition, the pore size can be continuously adjusted in the range of 2–50 nm, and the pores and the large and silan-rich surface (up to 2000 m²/g) are easy to modify (Gao et al., 2021a). Mesoporous molecular sieves are often used as carriers to load or dope transition metal (e.g., Zr and Hf) elements and rare earth elements into their frameworks, surfaces, or pores. There is no doubt that mesoporous materials have also shown their talents in the field of biomass catalytic upgrading (Table 2).

LA and its Esters as Substrates

Using LA as a reaction substrate, ZrO₂ was supported on typical hexagonal mesoporous Si, such as Mobil Composition of Matter-41 (MCM-41) and Santa Barbara Amorphous-15 (SBA-15) (entry 1, 2, 4 in Table 2) prepared by Kuwahara et al. (2014). The silicon carrier itself is inactive, and the reaction kinetics demonstrated that the pore size of mesoporous Si had little effect on the catalytic activity. However, it was possible to increase the CTH reaction activity by expanding the surface area of the oxide support carrier, which can change the local structure of the Zr species. Specifically, the high surface area of Si support provided a surface environment that was suitable for the introduction of highly dispersed low-coordination Zr. The loss of used catalytic activity was due to the strong adsorption of organic residues on the catalyst surface. This prevented the next batch of organic substrates from entering the Zr active site. Similar catalysts have also been reported, and the conversion and yield have been further improved (entry 3 of Table 2) (Kuwahara et al., 2017). For the conversion of EL to GVL, using biopolymer chitosan as a support to prepare the efficient Zr-containing catalyst (chitosan-Zr) was developed by Wang et al. (2020c). Chitosan is derived from the diacylation of chitin (Synowiecki and Al-Khateeb, 2003). The world's marine ecosystems produce about 1,600 million tons of chitin each year (Aydın and Aksoy, 2009). And it was the second kind of abundant biopolymer in nature after cellulose, but they were underutilized. Many-NH₂ and-OH groups exist in the chitosan, which means it has a strong chelating ability for M⁺. The conversion rate of the relevant

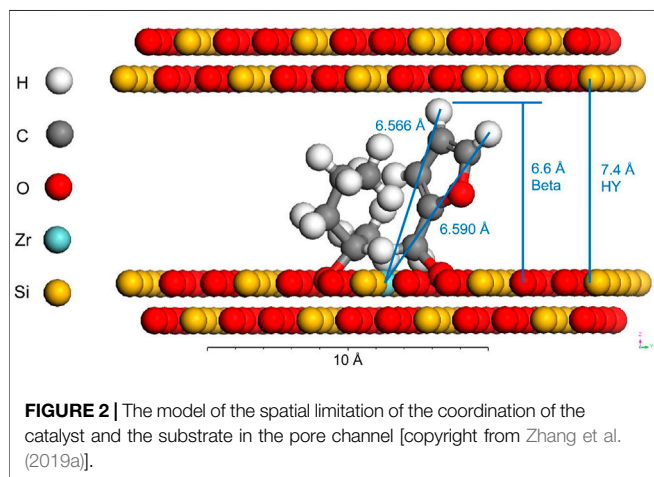
catalysts containing Zr or Hf can reach 100%, and the corresponding yield was 97% (entries 5 and 6 of Table 2). Undoubtedly, it was a wise strategy to use biomass-derived chemicals to prepare catalysts for the efficient valorization of biomass feedstocks.

FF as a Substrate

Using FF as the starting substrate, the same material had been studied with different Zr coatings of ZrO₂ using wet chemical methods (entry 7 of Table 2) (Iglesias et al., 2018). The first type was related to the strong acid position on the interface with Si. Another type of highly dispersed t-ZrO₂ crystals that were ubiquitous in the second and third layers was related to the position of the weak acid. This catalyst was used for the cascade reaction of FF to GVL. In addition, pyridine titration experiments during vacuum and 2-PrOH soaking were also carried out, proving that the Lewis acidity of all ZrO₂ monolayer thicknesses dominated the key role. A single ZrO₂ monolayer had a few Brønsted acid sites. And this may be related to residual surface silanol. The etherification and isomerization of FA to EL reduced the reaction rate. Fe₃O₄/ZrO₂@MCM-41 was tailored by the impregnation of ZrO₂ on mesoporous MCM-41 support coated by Fe₃O₄. It could efficiently catalyze the cascade reaction in terms of conversion of FF to GVL (entry 8 of Table 2) (Gao et al., 2021). The introduction of these two substances did not change the original ordered hexagonal framework of MCM-41. The incorporation of Fe₃O₄ was a simple way to adjust its acidity. The kinetic study demonstrated higher activation energy for the LA-to-GVL step (86.9 kJ/mol) than that of FF transfer hydrogenation (35.0 kJ/mol) and that of subsequent alcoholysis process (51.0 kJ/mol). The catalyst could be fully recovered and reused because of its excellent magnetic property. By Zr K-edge XAFS analysis, it can be seen that the Zr⁴⁺ oxide species anchored on the silica surface in a low-coordination state played the most important role in the reaction. Another application of this catalyst was the conversion of FF and 2-methylfuran (2-MF) to diesel precursors through the hydroxyalkylation/alkylation (HAA) reaction (Luo et al., 2018). The mesoporous catalyst was prepared by using ZrO₂ and phosphotungstic acid (TPA) on the inside and outside of the pores of SBA-15 (Srinivasa Rao et al., 2018) (entry 9 of Table 2). It has also been reported that Zr-SBA-15 performs average in

TABLE 3 | Zr/Hf-containing zeolite catalysts.

Entry	Substrate	Catalyst	Condition	H-donor	Product	Conv. (%)	Yield (%)	References
1	LA	Zr-Beta/Al-MFI-ns	120°C, 11 h	2-BuOH	GVL	100	96	Bui et al. (2013)
2	ML	Hf-Beta	160°C, -	2-BuOH	GVL	80	76.8	Luo et al. (2014)
3	EL	Zr-beat-100	150°C, 10 h	2-PrOH	GVL	100	96	Wang J. et al. (2014)
4	BL	(Zr)SSIE-beta	230°C, 24 h	2-BuOH	GVL	85	76	Antunes et al. (2016)
5	FF	Zr/Al-β-TUD1	120°C, -	2-BuOH	GVL	85	76	Antunes et al. (2016)
6	FF	Zr-HY/Al-HY	120°C, 5 h	2-PrOH	GVL	95	85	Zhang H. et al. (2019)
7	FF	Zr-Al-Beta	120°C, 3 h	2-PrOH	FA	99.6	97.3	Gao et al. (2020)



transforming FF to FA (Iglesias et al., 2015). However, it has excellent performance when reducing cyclic ketones with secondary alcohols. After the reaction, the corresponding alcohol yield was as high as 99% (entry 10 of Table 2).

ZR/HF-CONTAINING ZEOLITE CATALYSTS

Zeolite is a kind of nanoporous aluminosilicate crystal (Chai et al., 2021; Mardiana et al., 2022). Because of its regular pore structure and adjustable acidity, it is widely used in adsorption, separation, and catalysis (Sushkevich et al., 2014; Koreniuk et al., 2015; Wang et al., 2016c; Kim et al., 2020). The support material mainly uses mesoporous molecular sieves, which are used to provide templates to increase the stability and surface area of the catalyst, while zeolite will coordinate with the metal and form new bonds. As we all know, the catalytic activity of a molecular sieve is closely related to its unique acidity (Ramanathan et al., 2008; Melero et al., 2018; Cho et al., 2020). Usually, the acidity of zeolite is mostly affected by the isostructural substitution of Al^{3+} by Si^{4+} in the framework. This can create an imbalance of negative charges in the crystal lattice, and the concomitant exchangeable cations can make up for this imbalance (such as H^+ , Na^+ , K^+). When protons are connected to oxygen atoms

that are connected to silicon and Al atoms, the local charge transfer weakens and lengthens the O-H bond. In turn, this enhances the strength of its Brønsted acidity (Melero et al., 2017). The final result of these bonding interactions is that the local environment determines the type and intensity distribution of acidic sites. After a long-term research, scientists have found that if the concentration of substituted tetrahedral atoms does not exceed a certain threshold, Brønsted acid sites can show a constant acid strength which is suitable for adsorption and catalysis (Hernández et al., 2016). Therefore, the high intrinsic catalytic activity of zeolite is mainly derived from the excellent stability of the transition state in the nanopore confinement. Table 3 compares the catalytic effects of several different Zr/Hf-containing zeolite catalysts with the substrate as the classification standard.

LA and its Esters as Substrates

The reaction system of converting LA to GVL can use Zr-Beta and MFI topological structure nano-layer aluminosilicate (Al-MFI-ns) as the bicatalyst (entry 1 of Table 3) (Bui et al., 2013). Both of these steps resulted in the oxidation of the H-donor, which can be separated from the product. And it can be regenerated under mild gas-phase conditions and was directly put into use next time. It was noteworthy that this process can be achieved with cheap catalysts (e.g., Ni or Cu). Moreover, the combined catalysts can also convert hemicellulose to GVL. This also provides a new potential process for the transformation of pentoses to GVL.

The process of reducing ML to GVL by Lewis acid catalyst based on relevant kinetic parameters was described Luo et al. (2014). The reaction sequence and the rate of the mechanism were calculated. And the kinetic parameters of Ti, Sn, Zr, and Hf β -catalysts at different temperatures were analyzed (entry 2 of Table 3). Although the selectivity of GVL was over 94%, the turnover rate of these three zeolite catalysts was different during the MPV reaction process, and the Hf β catalyst had the highest activity. It is confirmed that the stronger the Lewis acid of the catalyst is, the more stable the six-membered ring transition state of the rate-limiting CTH step can be achieved (Assary et al., 2013). Kinetic studies were carried out by changing the H-donor (primary alcohol and secondary alcohol), proving that reducing the chain length of the alcohol did not affect the E_a .

TABLE 4 | Zr/Hf-containing MOF catalysts.

Entry	Substrate	Catalyst	Condition	H-donor	Product	Conv. (%)	Yield (%)	References
1	LA	ZrF-MOF	200°C, 2 h	2-PrOH	GVL	98	96	Yun et al. (2019)
2	LA	HPW@ MOF-808	160°C, 6 h	2-PrOH	GVL	99	87	Li et al. (2021a)
3	ML	UiO-66-S60	140°C, 9 h	2-BuOH	GVL	98	80	Kuwahara et al. (2016)
4	EL	UiO-66(Zr)	200°C, 2 h	2-PrOH	GVL	100	92.7	Valekar et al. (2016)
5	EL	Hf-MOF	120°C, 8 h	2-PrOH	GVL	99	94	Rojas-Buzo et al. (2018)
6	FF	DUT-67(Hf)	180°C, 24 h	2-PrOH	GVL	100	87.1	Li et al. (2019c)
7	FF	M-MOF-808	30°C, 24 h	2-PrOH	FA	94.2	90	Valekar et al. (2020)
8	FF	P/Zr-MOFs	200°C, 2 h	2-PrOH	FA	96.1	96	Wang Y. et al. (2020)

EL was catalytically reduced to GVL by Zr-Beta zeolite. A small amount of Zr (Si/Zr ~75–200) was incorporated into the zeolite (Wang et al. (2014a)). The Zr-Beta zeolite catalyst with isolated Zr atoms with Lewis acidity was prepared (entry 3 of **Table 3**). Density functional theory (DFT) calculation studies showed that Zr^{4+} was located in unique crystallographic positions of zeolite. To test its industrialization potential, the catalyst effect was further tested in the batch reactors and continuous flow reactors. Through the investigation of the mechanism, it was found that Brønsted acid sites can cause other side reactions. For example, the production of hemiacetals, pentenes, and their isomers reduced the selectivity to GVL.

FF as a Substrate

TUD-1 mixed with Zr/Al and zeolite β -type silicate catalyst was prepared and used for a series of conversion of FF (entry 4 and 5 of **Table 3**) (Antunes et al., 2016). Using 2-BuOH as an H-donor, a stepwise kinetic modeling study was successfully carried out. The effect of catalysts materials on intermediates selectivity was revealed. It was found that the Zr site played a decisive role in the reduction of FF to FA and levulinic acid (LE) to GVL. It was proved that the coexistence of Al sites can promote the acid catalysis step, involving the process of FA to alkyl furfuryl ethers (FEs), LEs, angelica lactones (AnLs), and LA, respectively. A similar combination also used the catalysts of Zr-HY (Lewis acid) and Al-HY (Brønsted acid) (Zhang et al. (2019a)). The Zr-containing zeolite is prepared by a post-synthesis method (entry 6 of **Table 3**). Zr was added after the dealumination of the parent Al-containing zeolite. However, the model shown in **Figure 2** exhibits that there is a certain dimensional limitation in the coordination of FF and 2-PrOH at the Zr Lewis acidic site in the pore channel. Besides, active sites of Zr-Al-Beta zeolites can be changed by mild alkaline treatment (e.g., LiOH, NaOH, KOH) (Gao et al., 2020). It is worth mentioning that alkaline treatment can improve recalcitrance to deactivation and coking, which is beneficial for the recycling of the catalyst.

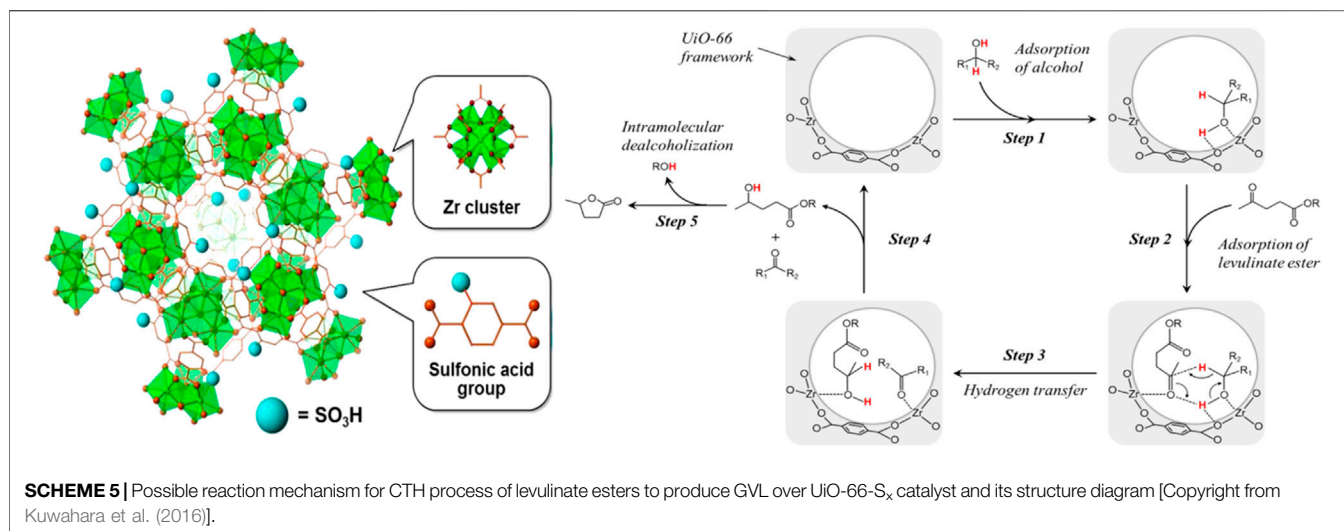
For the CTH conversion of FF to FA, 2-PrOH as the H-donor over cation-exchanged Lewis acidic BEA zeolite was calculated by DFT (Prasertsab et al., 2018). The catalytic activity of tetravalent

metal centers (Sn, Zr, and Hf) substituted into BEA. It found that in the order $Zr \geq Hf > Sn$, based on Ea.

In short, the binding capacity of the Hf-zeolite molecular sieve was better than that of the Zr-zeolite molecular sieve. This is because the activation energy of the Zr-zeolite reaction was lower when the Hf-zeolite molecular sieve catalyzed the reaction (Injongkol et al., 2017). The Zr-zeolite catalyst played an important role in the combination of stone and Zr/Hf to form the Lewis acid center, which was believed to constitute the active site of the catalyst. Moreover, it was further determined that this would play an important role in the adsorption and activation of the reactants. The Lewis acid site combined with the carbonyl group to activate the unsaturated C=O double bond, and finally formed the alcohol compound product.

ZR/HF-CONTAINING METAL-ORGANIC FRAMEWORK CATALYSTS

The term MOF was introduced in 1995 and was now widely accepted (Furukawa et al., 2013). It was a kind of coordination polymer material with good crystal form (Wang et al., 2016a; Goetjen et al., 2020). MOF catalysts have been developed successfully in the application of renewable energy and environmental fields, which have good design capabilities (Zhang et al., 2017; Lin et al., 2021; Mautschke and Llabres, 2021). Highly adjustable porosity and specific surface area, high density of accessible metal sites were the fascinating part of this material (Rui et al., 2021). The microporous zeolite material has diffusion limitations. But the MOF has a mesopore with a diameter of about 9.8 nm, facilitating the full diffusion and mixing of the various substances in the reaction. In terms of BET surface area, zeolite is about $200\text{--}500\text{ m}^2\text{ g}^{-1}$, while MOF is about $1,000\text{--}10,000\text{ m}^2\text{ g}^{-1}$ (Dhakshinamoorthy et al., 2011). Generally, the surface area and porosity of MOF were much higher than those of zeolite, but the chemical and thermal stability of MOFs are not as good as that of zeolite. Zr/Hf-containing MOFs catalysts can be seen everywhere in the field of the transfer hydrogenation of biomass-based carbonyl compounds. **Table 4** summarizes the reaction conditions and yields of some excellent Zr/Hf-containing MOF catalysts for the conversion of biomass-based chemicals.



LA and its Esters as Substrates

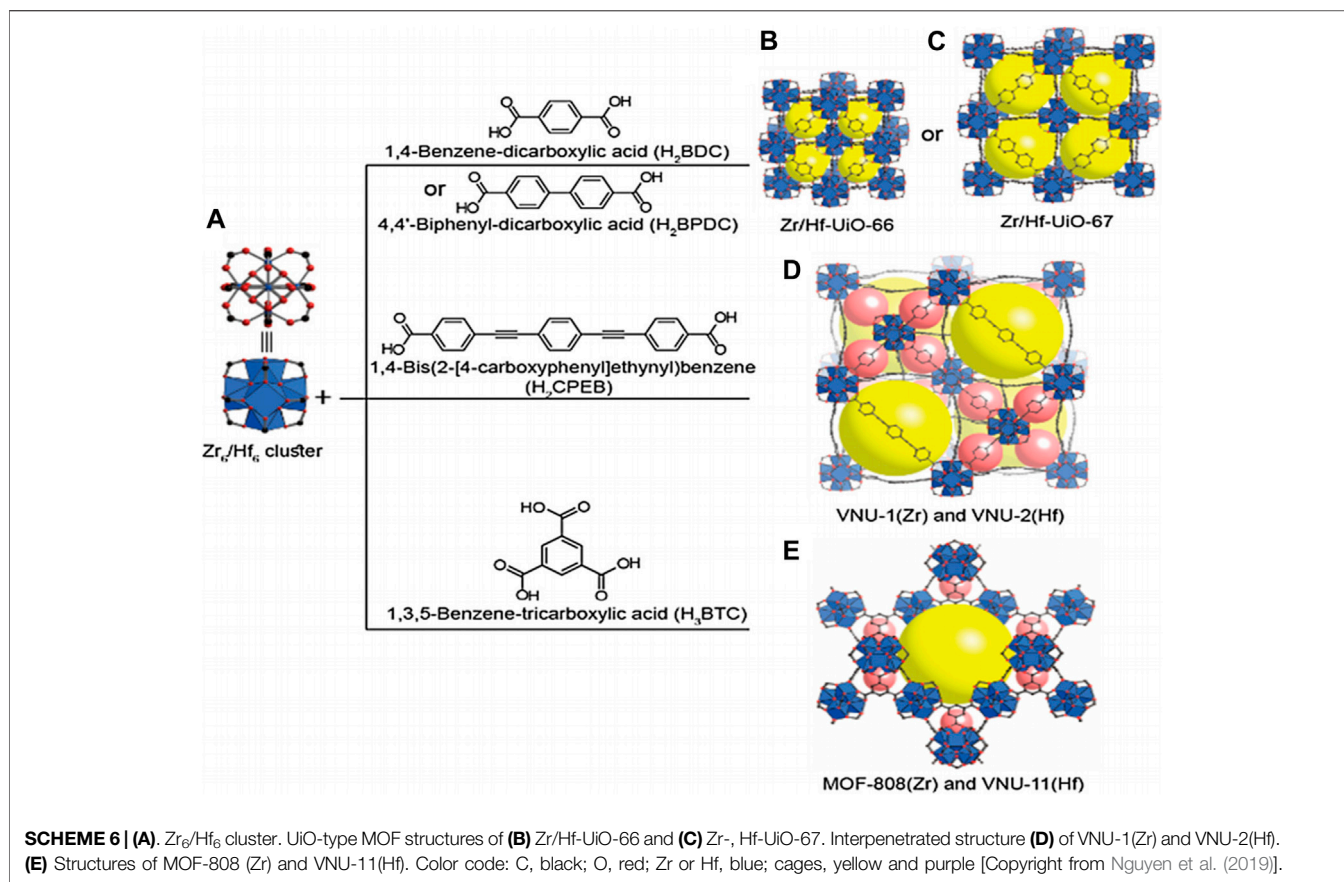
For the reaction of LA to GVL, Yun et al. avoided most of the toxic solvent dimethylformamide (DMF) which were typically used in the preparation of Zr polysulfide catalysts (Yun et al., 2019). Instead, they prepared the catalyst ZrF with fumaric acid and ZrCl₄ in water. In particular, they also used monocarboxylic acids as regulators, which affected the formation and morphology of aquatic zirconia, but did not affect its crystal structure and acidity. ZrF was adjusted with formic acid, acetic acid, and propionic acid, obtaining F-ZrF, A-ZrF, and P-ZrF, respectively. As a comparison, W-ZrF synthesized directly in water without a regulator and D-ZrF prepared in DMF in a traditional mode were also established. The order of particle size is F-ZrF (270 nm) > A-ZrF (130 nm) > P-ZrF (55 nm) > D-ZrF (25 nm). The size of ZrF was related to the molecular weight of the monocarboxylic acid. A regulator with a relatively low molecular weight can obtain ZrF with larger particle size and less excessive aggregation, which is beneficial for catalysis. W-ZrF without modifier did not have a good granular shape but existed in the form of a large block. Among them, at 200°C in 2 h, ZrF prepared by formic acid showed a 98% conversion of LA and 96% yield of GVL (entry 1 of **Table 4**).

HPW@MOF-808 was fabricated via a facile impregnation method with H₃PW₁₂O₄₀ and Zr-based MOF (Li et al., 2021a). Although MOF-808 had good activity in CTH reaction, its Brønsted acidity did not meet the requirements. Therefore, adding HPW (strong Brønsted acid) can effectively promote the esterification of LA with 2-PrOH and the subsequent lactonization reaction. Besides, MOF-808 had high acid resistance, which can exist stably in HCl and its cavity was large enough to encapsulate HPW. The yield of GVL can be obtained by reacting at 160°C for 6 h (entry 2 of **Table 4**), and the yield can be increased by 5% when the temperature was increased by 20°C. The dipping method for HPW@MOF-808 was relatively simple, but the preparation of MOF-808 was nearly a week, the process was complicated and time-consuming.

Expanding the starting material from LA to its ester, MOF material catalyst (e.g., sulfonic acid-functionalized UiO-66) also

performed well (entry 3 of **Table 4**) (Kuwahara et al., 2016). UiO-66(Zr) is comprised of 12-coordinated Zr₆O₄(OH)₄ clusters connected with 1,4-benzene dicarboxylate (BDC) linkers (Hu et al., 2016). Due to the very strong force between Zr-O, UiO-66(Zr) material has good water and thermal stability, and the structure can be maintained stably for a long time in a solution of pH = 1–11 (Shearer et al., 2014). Observing **Scheme 5**, it can be seen that each Zr-O cluster is 12-fold connected to adjacent clusters through a benzene dicarboxylate linker, and stacked together (Kuwahara et al., 2016). Correspondingly, it was confirmed that by FT-IR analysis, the Zr-O cluster only coordinated with the carboxylic acid oxygen atom, but not the sulfonated oxygen atom. With the increased degree of substitution of the sulfonic acid ligand, the XRD intensity and N₂ adsorption capacity of the microporous solid decreased significantly. In other words, the crystallinity and surface area of MOF materials decreased with the increase of sulfonic acid ligands, defects or irregular connections, and catalyst activity increased. Lewis basic sites (Zr₆O₄(OH)₄ cluster) catalyzed the CTH reaction of LA and its esters (entry 3 of **Table 4**). Brønsted-acid site (-SO₃H) promoted continuous intramolecular dealcoholization. The acid-base sites were arranged adjacent to each other in the confined nanospace, and had a synergistic effect on the entire reaction.

A variety of Zr-containing MOFs with different ligands were prepared for the conversion of EL to GVL (Valekar et al., 2016). UiO-66(Zr) showed good catalytic activity (92.7% GVL yield) at a high temperature (200°C), as shown in entry 4 of **Table 4**. In contrast, MOF-808 has been shown to produce GVL (85% yield) quickly at a moderate reaction temperature (130°C). It is worth mentioning that the latter also performed well in open systems using solvent reflux. In addition, through acid-base modification of the BDC ligand, the changes in its structure and catalytic effect were studied. It was found that the -COOH functional group can provide additional acidity, but the surface area and pore volume of the material have a considerable loss, and the presence of the -NH₂ group in the ligand provided additional alkalinity to the material, and the surface area loss was small. This was due to the



smaller size of the -NH₂ group compared to the -COOH group. The order of pore size and EL conversion and GVL yield showed consistency, that was UiO-66(Zr)-COOH (25% EL conversion, 13.9% GVL yield) < UiO-66(Zr)-NH₂ (99% EL conversion, 64.6% IPL yield) < UiO-66(Zr) (100% EL conversion, 92.7% GVL yield). The low catalytic efficiency of UiO-66(Zr)-COOH was because EL only reacted on its surface or diffused slowly into its narrow pores. On the contrary, when UiO-66(Zr)-NH₂ was used, almost all EL was converted, but the main by-product IPL was produced. This proved that UiO-66(Zr) functionalized with -NH₂ will preferentially undergo transesterification with excess 2-PrOH. Similar conversion and yield have been obtained in other work using the same substrate (entry 4 of **Table 4**) (Rojas-Buzo et al., 2018).

Using EL as the starting substrate, it can be directly converted to GVL through transfer hydrogenation. Sergio et al. prepared a series of materials such as UiO-66 and MOF-808, using formic acid as a modulator (Rojas-Buzo et al., 2018). The latter can be converted into GVL to obtain 100% FF conversion and 97% yield (2 h, 100°C), as shown in entry 5 of **Table 4**. Compared to UiO-66 (pore size 6 Å), MOF-808 has a wider pore structure (pore size 14 Å), which allows the conversion of larger substrates (Mautschke and Llabres, 2021). In the cascade reaction, the combination of Hf-MOF-808 with Al-Beta catalyst was used, and a 51% yield was obtained after 6 h of reaction (entry 5 of **Table 4**). Hf-MOF-808 showed excellent activity and specific

selectivity in hydrogenating carbonyl compounds through the CTH strategy because of its poor crystallinity, defects, large specific surface, and abundant Lewis acid-base sites. By using DFT calculations on the mechanism of MPV reaction, Lin et al. found that carbonyl compounds (e.g., ketones and alcohols) filled the defects of Hf-MOF (Lin et al., 2021). Lewis acid with Hf as the center can coordinate with the oxygen of the substrate molecule, and form a six-membered ring transition state. But other reactive groups with insufficient hardness or large steric hindrance (e.g., -NO₂, C=C, -CN) were difficult to coordinate with Hf, which was difficult to play a catalytic role. This also explained why Hf-MOF materials have specific selectivity for reducing carbonyl groups.

FF as a Substrate

For the reaction of FF to GVL, DUT-67 (Hf) performed well. All Hf⁴⁺ contained in the Hf₆O₈ cluster of 12-linked UiO-66(Hf) was saturated, so it is difficult to introduce SO₄²⁻ through a post-synthetic modification method (Li et al., 2019c). In contrast, each Hf cluster of DUT-67 (Hf) is 8 times connected to the 2,5-thiophenedicarboxylic acid (H₂TDC) linker (Bon et al., 2013). An inorganic acid (H₂SO₄) can be added to introduce Brønsted acid sites. The optimal ratio of sulfated DUT-67(Hf) can convert 100% of FF and undergo a cascade reaction (180°C for 20 h) to finally obtain 84.9% GVL (entry 6 of **Table 4**). However, the preparation process of the catalyst was very complicated and time-consuming, which was a challenge for the promotion of large-scale use.

TABLE 5 | Zr/Hf-containing metal-organic hydride catalysts.

Entry	Substrate	Catalyst	Condition	H- donor	Product	Conv. (%)	Yield (%)	References
1	LA	Hf-DTMP	140°C, 3 h	2-BuOH	GVL	98.7	96.9	Hu L. et al. (2019)
2	LA	Zr-BDB	130°C, 3 h	2-PrOH	GVL	99.7	97.2	Song et al. (2021)
3	ML	Zr-BDB	130°C, 4 h	2-PrOH	GVL	99.7	98.4	Song et al. (2021)
4	EL	Zr-BDB	130°C, 6 h	2-PrOH	GVL	99.5	98.7	Song et al. (2021)
5	EL	PPOA-Hf	160°C, 6 h	2-PrOH	GVL	100	85	Wu W. et al. (2018)
6	EL	HA-Zr	150°C, 24 h	2-PrOH	GVL	100	88.3	Xiao et al. (2017)
7	EL	Zr-SRf	150°C, 7 h	2-PrOH	GVL	92.4	92	Zhang et al. (2018)
8	EL	Zr-PhyA	200°C, 1 h	2-PrOH	GVL	100	98.5	Song et al. (2015b)
9	EL	Hf-ATMP	150°C, 4 h	2-PrOH	GVL	95	86	Xie et al. (2016)
10	EL	Zr-CA	150°C, 4 h	2-PrOH	GVL	100	96.9	Xue et al. (2016)
11	EL	FDCA-Hf	160°C, 4 h	2-PrOH	GVL	100	98	Li et al. (2018b)
12	EL	Zr-TMPA	160 °C, 8 h	2-PrOH	GVL	100	96.2	Xie et al. (2017)
13	EL	Zr-HBA	150°C, 4 h	2-PrOH	GVL	100	94.4	Song et al. (2015a)
14	EL	Hf-OFR	150°C, 9 h	2-PrOH	GVL	91	86	Chen et al. (2021a)
15	EL	Hf-GO	150°C, 5 h	2-PrOH	GVL	95.5	87.7	Li et al. (2020c)
16	EL	Hf-GO	150°C, 5 h	2-PrOH	GVL	54.8	54.7	Li et al. (2020c)
17	EL	Hf-DTMP	140°C, 3 h	2-BuOH	GVL	97.63	96.2	Hu L. et al. (2019)
18	BL	Zr-BDB	130°C, 6 h	2-PrOH	GVL	81.4	77.2	Song et al. (2021)
19	BL	ZrPO-1.00	210°C, 2 h	2-PrOH	GVL	98.1	95.7	Li et al. (2017)
20	FF	ZrPN	140°C, 2 h	2-PrOH	FA	98	98	Li et al. (2016c)
21	FF	Zr-LS	100°C, 1 h	2-PrOH	FA	97.5	96	Zhou et al. (2019b)
22	FF	Zr-LS	80°C, 3 h	2-PrOH	FA	99	90	Zhou et al. (2019b)
23	FF	PhP-Hf	120°C, 2 h	2-PrOH	FA	99.2	97.6	Li et al. (2019a)
24	FF	Zr-HAs	50°C, 15 h	2-PrOH	FA	97.4	96.9	Sha et al. (2017)
25	FF	Hf-TA	70°C, 3 h	2-PrOH	FA	100	99	Wang X. et al. (2020)
26	FF	Hf-DTMP	130°C, 3 h	2-BuOH	FA	99.9	98.5	Hu et al. (2019b)
27	FF	HPW/Zr-β	160°C, 24 h	2-PrOH	GVL	100	68	Winoto et al. (2019)
28	HMF	Hf-DTMP	100°C, 2 h	2-BuOH	BMHF	99	90	Hu et al. (2019b)
29	HMF	MZCCP	130°C, 4 h	2-BuOH	DHMF	83.9	64.2	Hu et al. (2018)

In the classic reaction of FF to FA under mild conditions, three Zr-molybdenum compounds (UiO-66, UiO-67, and DUT-52) with the same ligand-metal node coordination but different porous properties were compared. It was proved that the metal node connectivity was more important than high porosity when the Zr-porous membrane material underwent a CTH reaction (Valekar et al., 2020). In addition, the synthesis of an M-MOF-808 material has also been optimized, which can also obtain a 94.2% FF conversion and 90% FA yield after reacting at 40°C for 24 h (entry 7 of **Table 4**). Low-temperature conditions provided novel ideas for new applications of low-grade waste heat. P/Zr-MOF catalysts were prepared by (NH₄)₂HPO₄ pyrolysis approach starting from Zr-MOFs (Wang Y. et al., 2020). P/Zr-MOFs compared with Zr-MOFs, a part of O-Zr-O in the MOFs was phosphated to form O-Zr-P and P-Zr-P, in which Zr-P possessed stronger Lewis acidity and basicity than those of Zr-O. The increase of reaction temperature and time was conducive to the CTH of FF. However, too high a reaction temperature will result in a decrease in the conversion of FF. Meanwhile, too long reaction time will lead to side reactions of excessive hydrogenation and hydrogenolysis, resulting in a decrease in the selectivity of FA (entry 8 of **Table 4**).

In a word, Zr/Hf-containing MOFs exhibited good chemical, thermal, and mechanical stability due to the strong bond between Zr/Hf and oxygen and their high coordination number. **Scheme 6** clearly shows the proposed structure of MOFs built from 12-connected and 6-connected Zr₆/Hf₆ clusters coordinated with ditopic and tritopic carboxylate linkers, respectively (Nguyen et al., 2019).

ZR/HF-CONTAINING METAL-ORGANIC HYDRIDE CATALYSTS

Metal-organic hydride materials have also been known as unconventional MOF (UMOF) (Gagnon et al., 2012; Goetjen et al., 2020). Compared with the MOF material with good crystal form, Metal-organic hydrides are polymer with an amorphous structure but have good stability and more accessible sites. The organometallic coordination polymerization catalyst has high catalytic activity and good molecular tailoring (Wang et al., 2016b; Liu et al., 2021e). By adjusting the microstructure of catalysts, such as the substituents of the ligand, the coordination atom, and the electronic and three-dimensional environment of the coordination center, the molecular design and assembly of the polymer can be realized at the molecular level (Erickson et al., 2015; Hu et al., 2018; Liu et al., 2019; Peng et al., 2021). In this way, the physical properties of polymers can be controlled, and various polymers with novel functions and stereoisomers can be obtained (Asghari and Yoshida, 2006; Dutta et al., 2012; Jain et al., 2015; Zhou et al., 2019a). **Table 5** summarizes the reaction conditions and yields of some excellent Zr/Hf-containing metal-organic hydride catalysts for the conversion of biomass-based chemicals.

LA and its Esters as Substrates

Using LA as a substrate, a new type of organic zirconium borate (Zr-BDB) was developed by Song et al. to convert it to GVL (Song et al., 2021). 1,4-Benzodiboric acid (BDB) and ZrOCl₂·8H₂O were synthesized by a solvothermal method in DMF (entry 1 of

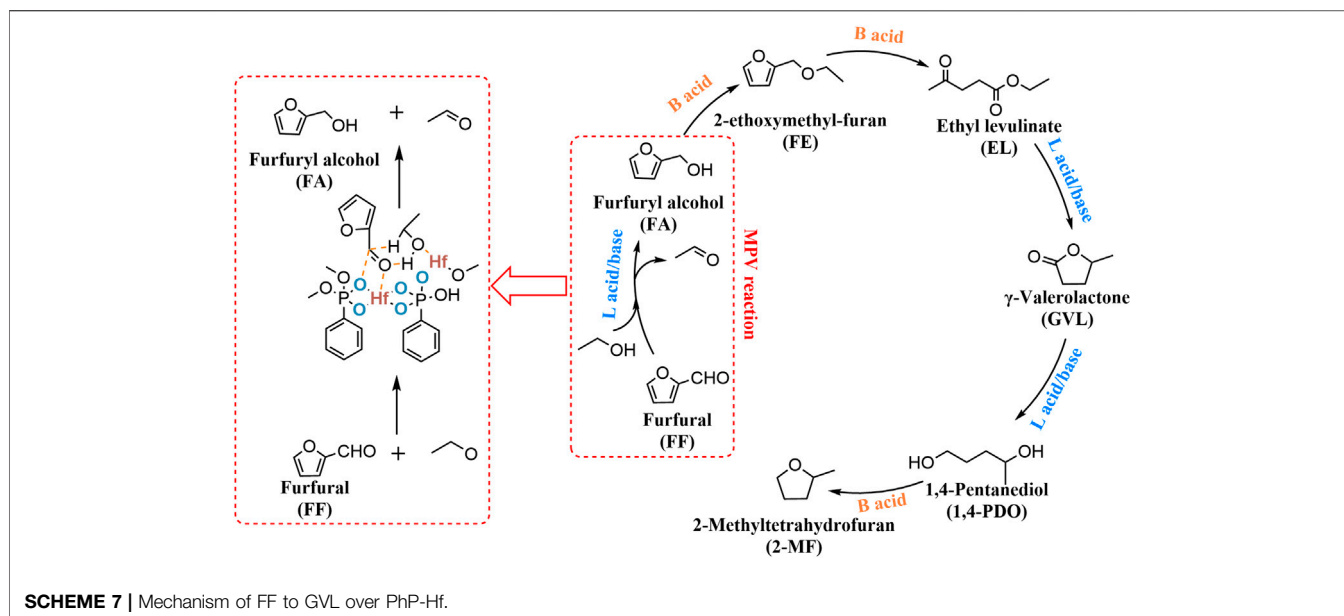


Table 5). As a Lewis acid, BDB can coordinate with and activate the hydroxyl group in alcohol. At the same time, Zr was combined to activate the carbon group, achieving the purpose of synergistically catalyzing the MPV reaction. The yields of different substrates (ML > EL > BL) to GVL were due to the increased steric hindrance from methyl to butyl.

In the system of EL to GVL, there were many different catalysts, such as Zr-BDB, PPOA-Hf, HA-Zr, Zr-SRf, Zr-PhyA, Hf-ATMP, Zr-CA, 2,5-furandicarboxylic acid (FDCA)-Hf, Zr-TMPA, Zr-HBA, Hf-OFR, Hf-GO, Hf-DTMP (entry 4–17 of **Table 5**). All of them were coordinated by different organic ligands. Hf-OFR was prepared by the oxytetracycline fermentation broth residue (OFR), which is an abundant solid waste in the fermentation industry (Chen et al., 2021a). It is beneficial for both pharmaceutical wastes and bio-based resources. Hazardous and tricky to treat. EL was completely converted to obtain GVL with a yield of 85% (160°C, 6 h) by PPOA-Hf catalyst (Wu et al., 2018b). Ea was estimated at approximately 53 kJ/mol, which was relatively lower than other catalysts. The layered metal phosphonate-phosphate hybrid can be used for ion exchange. Using humic acid (HAs) as a raw material to synthesize Zr-containing catalyst (Zr-HA) was proposed (Xiao et al., 2017). HAs are an important part of lignite (typical low-rank coal) with abundant reserves. This low-rank coal is usually only used as a low-quality fuel. If it can be applied to fine chemical catalysts, it will be a new method to realize the classification and clean utilization of coal. Similarly, HA and the solid residues (SR) after HA extraction from lignite were used to prepare Zr-SRf catalyst (Zhang et al., 2018). Compared to the previous study, this work had greatly shortened the reaction time (7 h V.S. 24 h) and improved the selectivity (83% V.S. 99.5%). Besides, graphene oxide (GO) is rich in acidic carboxyl groups and phenolic hydroxyl groups (Palermo et al., 2016; Karthik et al., 2021). Through the coordination of Hf⁴⁺/Zr⁴⁺ with the carboxyl

group in graphene oxide, Hf-GO, and Zr-GO catalysts were constructed (Li et al., 2020c).

There are not many studies on BL as the substrate, and zirconium phosphates were used in this reaction (Li et al., 2017). The BL conversion at 2 h was 98.1%, and the GVL yield was 95.7% (entry 19 of **Table 5**). Compared with ZrO₂, the binding energies of Zr3d and O1s of all ZrPO-X materials were significantly increased. This was due to the introduction of phosphorus, leading to the decrease of Zr electron density and the increase of surface hydroxyl groups.

FF as a Substrate

For the conversion of FF to FA, a template-free method to synthesize various heterogeneous acid–base bifunctional nitrogen-containing alkyltriphosphonate-metal hybrids (MPN) catalysts were synthesized by Li et al. (Li et al., 2016c). The organotriphosphate-zirconium hybrid (ZrPN) mainly focused on the CTH reactions of biomass-derived carbonyl compounds to alcohols and aldoses to ketoses (entry 20 of **Table 5**). Through calculation, the rate constant of ZrPN at 100°C was $3.6 \times 10^{-3} \text{ s}^{-1}$, which was 12 times than that of ZrO₂. The Ea of ZrPN and ZrO₂ were 70.5 and 79.1 kJ/mol, respectively. Both two proved the superior performance of the Zr N-Alkyltriphosphate nanohybrid from the perspective of reaction kinetics. It's worth paying high attention that the intramolecular CTH of C3–C6 aldoses to the corresponding ketoses in water was also studied. Generally, Al-zeolites can not catalyze glucose isomerization due to the weakening of Lewis acid sites existing in water. In contrast, Lewis acid sites in ZrPN can not be hampered by water, which showed excellent potential in CTH reaction. In another word, ZrPN can be extrapolated to other similar lignocellulose-derived substrates for upgrading biomass.

The conversion of FF can also be achieved by simply assembling lignosulfonate and ZrCl₄ to form a Zr-containing polyphenol biopolymer catalyst under hydrothermal conditions (entry 22 of **Table 5**) (Zhou et al., 2019b). Lignosulfonate has a sulfonic acid

group and can be used as an alkali-free acidic site. Therefore, dangerous sulfonation can be avoided. Catalytic experiments were also carried out with 18 typical aldehydes and ketones in the traditional chemical industry as substrates. It proved that Lignosulfonate-based catalysts had good universality and application potential. Different proportions of phenylphosphonic acid (PhP) and Hf were used to prepare the acid-base bifunctional nano-hybrid catalyst PhP-Hf, which can convert FF to FA (entry 23 of **Table 5**) (Li et al., 2019a). The catalyst had a moderate acid-base site and acidity. PhP-Hf was weaker than that of HfO_2 , but it also promoted the reaction. Acid (Hf^{4+}) and base (O^{2-}) sites had a synergistic effect on the CTH reaction of FF to FA. The base sites facilitated the adsorption and dissociation of 2-PrOH on the catalyst, and the aldehyde group was activated by Hf^{4+} . Then the six-membered ring transition state was formed *in situ* and completed the hydrogen transfer. And the E_a was calculated at about 60.8 kJ/mol.

The Hf-TA catalyst was synthesized in DMF with naturally occurring tannic acid (TA) as a ligand to coordinate with HfCl_4 . (Wang et al., 2020d). The advantage of this method was that renewable and natural resources were used to construct an efficient and environmentally friendly Hf-containing catalyst, and the preparation process was simple. Although the general catalyst can only be recycled about 5 times, the catalytic effectiveness of the 10th used catalyst was better than the first time. It was further confirmed by FT-IR spectra, showing that the residual DMF in the pore structure of the catalyst was gradually replaced by 2-PrOH during the reuse process. This would facilitate contact with more active sites, increasing the MPV activity. Under the relatively mild reaction conditions (70°C, 3 h), a high yield of 99.0% of FA can be obtained (entry 25 of **Table 5**). Zirconium phosphonate The materials synthesized by the coordination of organic acids and zirconium were widely used in the biomass-based conversion. Zr-containing catalysts such as Zr-HAs, Zr-DTMP, HPW/Zr- β (entries 24, 26, 27 of **Table 5**) also can be used in similar systems from FF to FA or GVL. By regulating the ratio of organic phosphonate and inorganic phosphate with the center of Zr metal (Silbernagel et al., 2016), further optimization of the MPV reduction reaction system could be successfully carried out. The specific active sites required for each step of FF to GVL were shown in **Scheme 7**. Lewis acid/base sites were responsible for the MPV reduction (FF to FA, and EL to GVL), while Brønsted acid sites exhibited key effects on the etherification reaction (FA to FE) and ring-opening reaction (FE to EL).

HMF as a Substrate

Converting HMF to BHMF is also a significant path for biomass-derived conversion. A new Hf-based metal-organic coordination polymer (Hf-DTMP) was assembled by HfCl_4 and diethylene triaminepenta (methylene phosphonic acid) (DTMP) (Hu et al., 2019b). The mechanism was that 2-BuOH, and HMF were first adsorbed on catalyst. Subsequently, 2-BuOH was dissociated into the active H and alkoxide by O^{2-} . Meanwhile, the carbonyl group of HMF was activated by Hf^{4+} . Then, a six-membered intermediate was generated by the dissociated alcohol and carbonyl group with $\text{Hf}^{4+}\text{-O}^{2-}$. Finally, BHMF was eventually

formed *via* CTH (entry 28 of **Table 5**). In contrast, the magnetic catalysts (MZCCP) synthesized by ZrCl_4 , cyanuric acid (CA), and Fe_3O_4 did not have an advantage in terms of yield (90% V.S. 64.2%) (entry 29 of **Table 5**) (Hu et al., 2018).

CONCLUSION AND PERSPECTIVES

Mountains of researches proved that CTH is a significant strategy to transform biomass-based substrates into chemical platform products and fuel precursors of high value. Zr/Hf can be supported on other materials or coordinated/coupled with them to form Zr/Hf-containing materials, of which they can play a significant role in CTH that is similar to noble metal catalysis. In this review, the catalytic effects and mechanisms of different types of Zr/Hf-containing catalysts are discussed. Various kinds of materials demonstrate different properties and preparation methods. Zr/Hf-containing oxides are relatively inexpensive and easily available. However, their basic sites are not strong and are easily affected by solvents, and the corresponding reaction activity is not ideal. Supported catalysts containing Zr/Hf can use existing templates to enhance stability and increase surface area. The zeolite catalysts are prone to be affected by the hydroxyl groups on Si, and the acidic enhancement of Lewis can effectively fix the metal and coordinate. The MOF catalysts generally have a good crystal form and spatial structure. However, the preparation process of these three catalysts is complicated and the relevant precursors are expensive, which is not suitable to apply from an economic point of view. Relatively speaking, the preparation steps of metal-organic hybrid materials are simpler and the time is shorter, which have abundant sources and room for expansion.

To establish a mature industrialization system, economic benefits and environmental impacts should be taken into account. In other words, the preparation and reaction process of the catalyst should be as simple and time-saving as possible. Also, the consumption of raw materials and energy should be low. Correspondingly, the purity and quality of the obtained product should be high. The problem at this stage is that there are seasonal differences in the availability of biomass raw materials, and the competitiveness of economic benefits is not very strong. As the saying goes, there is no useless waste, only misplaced resources. How to convert this huge amount of useless waste into resources that can replace the heavily polluting traditional energy and generate economic benefits is a problem that needs to be tackled on the road to green development. And this depends on the joint efforts of scientific researchers, enterprises, and the government, respectively. We still need to propose a new solid acid catalyst design strategy. 1) Using non-precious metal materials and green solvents to achieve a win-win situation for the economy and environmental protection. 2) Increasing the density of acid and base sites accessible to the catalyst. 3) Controlling the ratio of Lewis/Brønsted acid sites. 4) Developing more functional group synergistic catalysis. 5) Modulating the wettability of the catalyst surface together with increasing its water resistance. 6) Simplifying the catalyst preparation process, reducing the preparation cost, and controlling the energy consumption of each link accurately.

AUTHOR CONTRIBUTIONS

Writing—original draft preparation, YL Revising—manuscript, XL Figure drawing, ML Writing—reviewing, YM Data curation, JL Editing, ZZ Writing—reviewing, supervision, HZ All authors have read and agreed to the published version of the manuscript.

REFERENCES

- Abomohra, A. E.-F., Elsayed, M., Esakkimuthu, S., El-Sheekh, M., and Hanelt, D. (2020). Potential of Fat, Oil and Grease (Fog) for Biodiesel Production: A Critical Review on the Recent Progress and Future Perspectives. *Prog. Energy Combustion Sci.* 81, 100868. doi:10.1016/j.pecs.2020.100868
- Ahmad, S. F. K., Md Ali, U. F., and Isa, K. M. (2019). Compilation of Liquefaction and Pyrolysis Method Used for Bio-Oil Production from Various Biomass: A Review. *Environ. Eng. Res.* 25, 18–28. doi:10.4491/eeer.2018.419
- Ajmi, A. N., and Inglesi-Lotz, R. (2020). Biomass Energy Consumption and Economic Growth Nexus in OECD Countries: A Panel Analysis. *Renew. Energ.* 162, 1649–1654. doi:10.1016/j.renene.2020.10.002
- Antunes, M. M., Lima, S., Neves, P., Magalhães, A. L., Fazio, E., Neri, F., et al. (2016). Integrated Reduction and Acid-Catalysed Conversion of Furfural in Alcohol Medium Using Zr,Al-Containing Ordered Micro/mesoporous Silicates. *Appl. Catal. B: Environ.* 182, 485–503. doi:10.1016/j.apcatb.2015.09.053
- Asghari, F. S., and Yoshida, H. (2006). Dehydration of Fructose to 5-hydroxymethylfurfural in Sub-critical Water over Heterogeneous Zirconium Phosphate Catalysts. *Carbohydr. Res.* 341, 2379–2387. doi:10.1016/j.carres.2006.06.025
- Assary, R. S., Curtiss, L. A., and Dumesic, J. A. (2013). Exploring Meerwein-Ponndorf-Verley Reduction Chemistry for Biomass Catalysis Using a First-Principles Approach. *ACS Catal.* 3, 2694–2704. doi:10.1021/cs400479m
- Atwoli, L., Baqui, A. H., Benfield, T., Bosurgi, R., Godlee, F., Hancocks, S., et al. (2021). Call for Emergency Action to Limit Global Temperature Increases, Restore Biodiversity, and Protect Health. *Med. J. Aust.* 215, 210–212. doi:10.5694/mja2.51221
- Aydn, Y. A., and Aksoy, N. D. (2009). Adsorption of Chromium on Chitosan: Optimization, Kinetics and Thermodynamics. *Chem. Eng. J.* 151, 188–194. doi:10.1016/j.cej.2009.02.010
- Bogale, T. F., Gul, I., Wang, L., Deng, J., Chen, Y., Majerić-Elenkov, M., et al. (2019). Biodegradation of 1,2,3-trichloropropane to Valuable (S)-2,3-dcp Using a One-Pot Reaction System. *Catalysts* 10, 3. doi:10.3390/catal10010003
- Bon, V., Senkovska, I., Baburin, I. A., and Kaskel, S. (2013). Zr- and Hf-Based Metal-Organic Frameworks: Tracking Down the Polymorphism. *Cryst. Growth Des.* 13, 1231–1237. doi:10.1021/cg301691d
- Brauer, M., Casadei, B., Harrington, R. A., Kovacs, R., Sliwa, K., Davaakhuu, N., et al. (2021). Taking a Stand against Air Pollution - the Impact on Cardiovascular Disease. *Eur. Heart J.* 42, 1460–1463. doi:10.1093/eurheartj/ehaa1025
- Brethauer, S., and Studer, M. H. (2015). Biochemical Conversion Processes of Lignocellulosic Biomass to Fuels and Chemicals - a Review. *Chimia* 69, 572–581. doi:10.2533/chimia.2015.572
- Bui, L., Luo, H., Gunther, W. R., and Román-Leshkov, Y. (2013). Domino Reaction Catalyzed by Zeolites with Bronsted and Lewis Acid Sites for the Production of γ -Valerolactone from Furfural. *Angew. Chem. Int. Ed.* 52, 8022–8025. doi:10.1002/anie.201302575
- Cao, W., Luo, W., Ge, H., Su, Y., Wang, A., and Zhang, T. (2017). UiO-66 Derived Ru/ZrO₂@C as a Highly Stable Catalyst for Hydrogenation of Levulinic Acid to γ -valerolactone. *Green. Chem.* 19, 2201–2211. doi:10.1039/c7gc00512a
- Chai, Y., Dai, W., Wu, G., Guan, N., and Li, L. (2021). Confinement in a Zeolite and Zeolite Catalysis. *Acc. Chem. Res.* 54, 2894–2904. doi:10.1021/acs.accounts.1c00274
- Champness, N. R. (2011). The Future of Metal-Organic Frameworks. *Dalton Trans.* 40, 10311–10315. doi:10.1039/c1dt11184a
- Chen, S., Wojcieszak, R., Dumeignil, F., Marceau, E., and Royer, S. (2018). How Catalysts and Experimental Conditions Determine the Selective Hydroconversion of Furfural and 5-hydroxymethylfurfural. *Chem. Rev.* 118, 11023–11117. doi:10.1021/acs.chemrev.8b00134
- Chen, Y., Yao, X., Wang, X., Zhang, X., Zhou, H., He, R., et al. (2021). Direct Use of the Solid Waste from Oxytetracycline Fermentation Broth to Construct Hf-Containing Catalysts for Meerwein-Ponndorf-Verley Reactions. *RSC Adv.* 11, 13970–13979. doi:10.1039/d1ra01738a
- Chen, Y., Zhang, L., Yang, Y., Pang, B., Xu, W., Duan, G., et al. (2021). Recent Progress on Nanocellulose Aerogels: Preparation, Modification, Composite Fabrication, Applications. *Adv. Mater.* 33, 2005569. doi:10.1002/adma.202005569
- Chia, M., and Dumesic, J. A. (2011). Liquid-phase Catalytic Transfer Hydrogenation and Cyclization of Levulinic Acid and its Esters to γ -valerolactone over Metal Oxide Catalysts. *Chem. Commun.* 47, 12233–12235. doi:10.1039/c1cc14748j
- Cho, H. J., Kim, D., and Xu, B. (2020). Selectivity Control in Tandem Catalytic Furfural Upgrading on Zeolite-Encapsulated Pt Nanoparticles through Site and Solvent Engineering. *ACS Catal.* 10, 4770–4779. doi:10.1021/acscatal.0c00472
- Choi, J. H., Mao, Y., and Chang, J. P. (2011). Development of Hafnium Based High-K Materials-A Review. *Mater. Sci. Eng. R: Rep.* 72, 97–136. doi:10.1016/j.mser.2010.12.001
- Crabtree, R. H. (2019). Transfer Hydrogenation with Glycerol as H-Donor: Catalyst Activation, Deactivation and Homogeneity. *ACS Sustain. Chem. Eng.* 7, 15845–15853. doi:10.1021/acssuschemeng.9b00228
- Dabros, T. M. H., Stummann, M. Z., Høj, M., Jensen, P. A., Grunwaldt, J.-D., Gabrielsen, J., et al. (2018). Transportation Fuels from Biomass Fast Pyrolysis, Catalytic Hydrodeoxygenation, and Catalytic Fast Hydrolysis. *Prog. Energy Combustion Sci.* 68, 268–309. doi:10.1016/j.pecs.2018.05.002
- Delgado, J., Vasquez Salcedo, W. N., Bronzetti, G., Casson Moreno, V., Mignot, M., Legros, J., et al. (2022). Kinetic Model Assessment for the Synthesis of γ -valerolactone from N-Butyl Levulinate and Levulinic Acid Hydrogenation over the Synergy Effect of Dual Catalysts Ru/C and Amberlite IR-120. *Chem. Eng. J.* 430, 133053. doi:10.1016/j.cej.2021.133053
- Dhakshinamoorthy, A., Alvaro, M., Corma, A., and Garcia, H. (2011). Delineating Similarities and Dissimilarities in the Use of Metal Organic Frameworks and Zeolites as Heterogeneous Catalysts for Organic Reactions. *Dalton Trans.* 40, 6344–6360. doi:10.1039/c1dt10354g
- Dutta, A., Patra, A. K., Dutta, S., Saha, B., and Bhaumik, A. (2012). Hierarchically Porous Titanium Phosphate Nanoparticles: An Efficient Solid Acid Catalyst for Microwave Assisted Conversion of Biomass and Carbohydrates into 5-hydroxymethylfurfural. *J. Mater. Chem.* 22, 14094. doi:10.1039/c2jm30623a
- Dutta, S., Yu, I. K. M., Tsang, D. C. W., Ng, Y. H., Ok, Y. S., Sherwood, J., et al. (2019). Green Synthesis of Gamma-Valerolactone (Gvl) through Hydrogenation of Biomass-Derived Levulinic Acid Using Non-noble Metal Catalysts: A Critical Review. *Chem. Eng. J.* 372, 992–1006. doi:10.1016/j.cej.2019.04.199
- Erickson, K. A., Stelmach, J. P. W., Mucha, N. T., and Waterman, R. (2015). Zirconium-catalyzed Amine Borane Dehydrocoupling and Transfer Hydrogenation. *Organometallics* 34, 4693–4699. doi:10.1021/acs.organomet.5b00415
- Furukawa, H., Cordova, K. E., O'Keeffe, M., and Yaghi, O. M. (2013). The Chemistry and Applications of Metal-Organic Frameworks. *Science* 341, 1230444. doi:10.1126/science.1230444
- Gagnon, K. J., Perry, H. P., and Clearfield, A. (2012). Conventional and Unconventional Metal-Organic Frameworks Based on Phosphonate Ligands: Mofs and Umofs. *Chem. Rev.* 112, 1034–1054. doi:10.1021/cr2002257
- Gao, G., Jiang, Z., and Hu, C. (2021). Selective Hydrogenation of the Carbonyls in Furfural and 5-hydroxymethylfurfural Catalyzed by Pt_{ni} alloy Supported on SBA-15 in Aqueous Solution under Mild Conditions. *Front. Chem.* 9, 759512. doi:10.3389/fchem.2021.759512
- Gao, L., Li, G., Sheng, Z., Tang, Y., and Zhang, Y. (2020). Alkali-metal-ions Promoted Zr-Al-Beta Zeolite with High Selectivity and Resistance to Coking in

FUNDING

The authors appreciate the financial support from the National Natural Science Foundation of China (21908033), Fok Ying-Tong Education Foundation (161030), Natural Science Special Foundation of Guizhou University ((2021)16 Special Post B), and GZU (Guizhou University) Found for Cultivation ((2020)73).

- the Conversion of Furfural toward Furfural Alcohol. *J. Catal.* 389, 623–630. doi:10.1016/j.jcat.2020.07.002
- Gao, X., Yu, X., Peng, L., He, L., and Zhang, J. (2021). Magnetic Fe₃O₄ Nanoparticles and ZrO₂-Doped Mesoporous MCM-41 as a Monolithic Multifunctional Catalyst for γ -valerolactone Production Directly from Furfural. *Fuel* 300, 120996. doi:10.1016/j.fuel.2021.120996
- Gawade, A. B., Tiwari, M. S., and Yadav, G. D. (2016). Biobased Green Process: Selective Hydrogenation of 5-Hydroxymethylfurfural to 2,5-Dimethyl Furan under Mild Conditions Using Pd-Cs₂.5H₀.5PW12O₄₀/K-10 Clay. *ACS Sustain. Chem. Eng.* 4, 4113–4123. doi:10.1021/acssuschemeng.6b00426
- Gilkey, M. J., and Xu, B. (2016). Heterogeneous Catalytic Transfer Hydrogenation as an Effective Pathway in Biomass Upgrading. *ACS Catal.* 6, 1420–1436. doi:10.1021/acscatal.5b02171
- Goetjen, T. A., Liu, J., Wu, Y., Sui, J., Zhang, X., Hupp, J. T., et al. (2020). Metal-organic Framework (Mof) Materials as Polymerization Catalysts: A Review and Recent Advances. *Chem. Commun.* 56, 10409–10418. doi:10.1039/d0cc03790g
- Gonell, F., Boronat, M., and Corma, A. (2017). Structure-reactivity Relationship in Isolated Zr Sites Present in Zr-Zeolite and ZrO₂ for the Meerwein-Ponndorf-Verley Reaction. *Catal. Sci. Technol.* 7, 2865–2873. doi:10.1039/c7cy00567a
- Han, X., Guo, Y., Liu, X., Xia, Q., and Wang, Y. (2019). Catalytic Conversion of Lignocellulosic Biomass into Hydrocarbons: A Mini Review. *Catal. Today* 319, 2–13. doi:10.1016/j.cattod.2018.05.013
- Hao, W., Li, W., Tang, X., Zeng, X., Sun, Y., Liu, S., et al. (2016). Catalytic Transfer Hydrogenation of Biomass-Derived 5-hydroxymethyl Furfural to the Building Block 2,5-bishydroxymethyl Furan. *Green. Chem.* 18, 1080–1088. doi:10.1039/c5gc01221j
- He, J., Li, H., Liu, Y., Zhao, W., Yang, T., Xue, W., et al. (2016a). Catalytic Transfer Hydrogenation of Ethyl Levulinate into γ -valerolactone over Mesoporous Zr/B Mixed Oxides. *J. Ind. Eng. Chem.* 43, 133–141. doi:10.1016/j.jiec.2016.07.059
- He, J., Li, H., Lu, Y.-M., Liu, Y.-X., Wu, Z.-B., Hu, D.-Y., et al. (2016b). Cascade Catalytic Transfer Hydrogenation-Cyclization of Ethyl Levulinate to γ -valerolactone with Al-Zr Mixed Oxides. *Appl. Catal. A: Gen.* 510, 11–19. doi:10.1016/j.apcata.2015.10.049
- Heard, C. J., Hu, C., Skoglundh, M., Creaser, D., and Grönbeck, H. (2016). Kinetic Regimes in Ethylene Hydrogenation over Transition-Metal Surfaces. *ACS Catal.* 6, 3277–3286. doi:10.1021/acscatal.5b02708
- Hengne, A. M., Malawadkar, A. V., Biradar, N. S., and Rode, C. V. (2014). Surface Synergism of an Ag-Ni/ZrO₂ Nanocomposite for the Catalytic Transfer Hydrogenation of Bio-Derived Platform Molecules. *RSC Adv.* 4, 9730–9736. doi:10.1039/c3ra46495d
- Hengne, A. M., and Rode, C. V. (2012). Cu-ZrO₂ Nanocomposite Catalyst for Selective Hydrogenation of Levulinic Acid and its Ester to γ -valerolactone. *Green. Chem.* 14, 1064–1072. doi:10.1039/c2gc16558a
- Hernández, B., Iglesias, J., Morales, G., Paniagua, M., López-Aguado, C., García Fierro, J. L., et al. (2016). One-pot cascade Transformation of Xylose into γ -valerolactone (GVL) over Bifunctional Brønsted-Lewis Zr-Al-Beta Zeolite. *Green. Chem.* 18, 5777–5781. doi:10.1039/c6gc01888b
- Hou, P., Ma, M., Zhang, P., Cao, J., Liu, H., Xu, X., et al. (2021). Catalytic Transfer Hydrogenation of Furfural to Furfuryl Alcohol Using Easy-To-Separate Core-Shell Magnetic Zirconium Hydroxide. *New J. Chem.* 45, 2715–2722. doi:10.1039/d0nj05638c
- Hu, D., Xu, H., Wu, Z., Zhang, M., Zhao, Z., Wang, Y., et al. (2021). Noble Metal-free Hierarchical ZrY Zeolite Efficient for Hydrogenation of Biomass-Derived Levulinic Acid. *Front. Chem.* 9, 725175. doi:10.3389/fchem.2021.725175
- Hu, F., Wang, Y., Xu, S., Zhang, Z., Chen, Y., Fan, J., et al. (2019). Efficient and Selective Ni/Al₂O₃-C Catalyst Derived from Metal-Organic Frameworks for the Hydrogenation of Furfural to Furfuryl Alcohol. *Catal. Lett.* 149, 2158–2168. doi:10.1007/s10562-019-02766-y
- Hu, L., Dai, X., Li, N., Tang, X., and Jiang, Y. (2019). Highly Selective Hydrogenation of Biomass-Derived 5-hydroxymethylfurfural into 2,5-bis(hydroxymethyl)furan over an Acid-Base Bifunctional Hafnium-Based Coordination Polymer Catalyst. *Sustain. Energy Fuels* 3, 1033–1041. doi:10.1039/c8se00545a
- Hu, L., Li, T., Xu, J., He, A., Tang, X., Chu, X., et al. (2018). Catalytic Transfer Hydrogenation of Biomass-Derived 5-hydroxymethylfurfural into 2,5-dihydroxymethylfuran over Magnetic Zirconium-Based Coordination Polymer. *Chem. Eng. J.* 352, 110–119. doi:10.1016/j.cej.2018.07.007
- Hu, L., Yang, M., Xu, N., Xu, J., Zhou, S., Chu, X., et al. (2017). Selective Transformation of Biomass-Derived 5-hydroxymethylfurfural into 2,5-dihydroxymethylfuran via Catalytic Transfer Hydrogenation over Magnetic Zirconium Hydroxides. *Korean J. Chem. Eng.* 35, 99–109. doi:10.1007/s11814-017-0238-3
- Hu, Z., Peng, Y., Gao, Y., Qian, Y., Ying, S., Yuan, D., et al. (2016). Direct Synthesis of Hierarchically Porous Metal-Organic Frameworks with High Stability and Strong Brønsted Acidity: The Decisive Role of Hafnium in Efficient and Selective Fructose Dehydration. *Chem. Mater.* 28, 2659–2667. doi:10.1021/acs.chemmater.6b00139
- Huang, R., Cui, Q., Yuan, Q., Wu, H., Guan, Y., and Wu, P. (2018). Total Hydrogenation of Furfural over Pd/Al₂O₃ and Ru/ZrO₂ Mixture under Mild Conditions: Essential Role of Tetrahydrofurfural as an Intermediate and Support Effect. *ACS Sustain. Chem. Eng.* 6, 6957–6964. doi:10.1021/acssuschemeng.8b00801
- Iglesias, J., Martínez-Salazar, I., Maireles-Torres, P., Martín Alonso, D., Mariscal, R., and López Granados, M. (2020). Advances in Catalytic Routes for the Production of Carboxylic Acids from Biomass: A Step Forward for Sustainable Polymers. *Chem. Soc. Rev.* 49, 5704–5771. doi:10.1039/d0cs00177e
- Iglesias, J., Melero, J. A., Morales, G., Paniagua, M., Hernández, B., Osatiashtiani, A., et al. (2018). ZrO₂-SBA-15 Catalysts for the One-Pot cascade Synthesis of GVL from Furfural. *Catal. Sci. Technol.* 8, 4485–4493. doi:10.1039/c8cy01121d
- Iglesias, J., Melero, J., Morales, G., Moreno, J., Segura, Y., Paniagua, M., et al. (2015). Zr-SBA-15 Lewis Acid Catalyst: Activity in Meerwein Ponndorf Verley Reduction. *Catalysts* 5, 1911–1927. doi:10.3390/catal5041911
- Injongkol, Y., Maihom, T., Treesukul, P., Sirijaraensre, J., Boekfa, B., and Limtrakul, J. (2017). Theoretical Study on the Reaction Mechanism of Hydrogenation of Furfural to Furfuryl Alcohol on Lewis Acidic Be Zeolites: Effects of Defect Structure and Tetravalent Metals Substitution. *Phys. Chem. Chem. Phys.* 19, 24042–24048. doi:10.1039/c7cp04229a
- Iriondo, A., Mendiguren, A., Güemez, M. B., Reques, J., and Cambra, J. F. (2017). 2,5-DMF Production through Hydrogenation of Real and Synthetic 5-HMF over Transition Metal Catalysts Supported on Carriers with Different Nature. *Catal. Today* 279, 286–295. doi:10.1016/j.cattod.2016.02.019
- Ishikawa, S., Jones, D. R., Iqbal, S., Reece, C., Morgan, D. J., Willcock, D. J., et al. (2017). Identification of the Catalytically Active Component of Cu-Zr-O Catalyst for the Hydrogenation of Levulinic Acid to γ -valerolactone. *Green. Chem.* 19, 225–236. doi:10.1039/c6gc02598f
- Jain, A., Shore, A. M., Jonnalagadda, S. C., Ramanujachary, K. V., and Mugweru, A. (2015). Conversion of Fructose, Glucose and Sucrose to 5-Hydroxymethyl-2-Furfural over Mesoporous Zirconium Phosphate Catalyst. *Appl. Catal. A: Gen.* 489, 72–76. doi:10.1016/j.apcata.2014.10.020
- Jiang, S., Li, F., Huang, J., Wang, Y., Lu, S., Li, P., et al. (2020). Catalytic Transfer Hydrogenation of Furfural over Magnetic Carbon-Encapsulated CoO@C Catalyst. *Chemistryselect* 5, 9883–9892. doi:10.1002/slct.202002269
- Jin, W., Pastor-Pérez, L., Shen, D., Sepúlveda-Escribano, A., Gu, S., and Ramirez Reina, T. (2019). Catalytic Upgrading of Biomass Model Compounds: Novel Approaches and Lessons Learnt from Traditional Hydrodeoxygenation - a Review. *ChemCatChem* 11, 924–960. doi:10.1002/cctc.201801722
- Karthik, V., Selvakumar, P., Senthil Kumar, P., Vo, D.-V. N., Gokulakrishnan, M., Keerthana, P., et al. (2021). Graphene-based Materials for Environmental Applications: A Review. *Environ. Chem. Lett.* 19, 3631–3644. doi:10.1007/s10311-021-01262-3
- Kerkel, F., Markiewicz, M., Stolte, S., Müller, E., and Kunz, W. (2021). The green Platform Molecule Gamma-Valerolactone - Ecotoxicity, Biodegradability, Solvent Properties, and Potential Applications. *Green. Chem.* 23, 2962–2976. doi:10.1039/d0gc04353b
- Khan, K., Tareen, A. K., Iqbal, M., Shi, Z., Zhang, H., and Guo, Z. (2021). Novel Emerging Graphdiyne Based Two Dimensional Materials: Synthesis, Properties and Renewable Energy Applications. *Nano Today* 39, 101207. doi:10.1016/j.nantod.2021.101207
- Kim, K. D., Kim, J., Teoh, W. Y., Kim, J.-C., Huang, J., and Ryo, R. (2020). Cascade Reaction Engineering on Zirconia-Supported Mesoporous MFI Zeolites with Tunable Lewis-Brønsted Acid Sites: a Case of the One-Pot Conversion of Furfural to γ -valerolactone. *RSC Adv.* 10, 35318–35328. doi:10.1039/d0ra06915a
- Koreniuk, A., Maresz, K., and Mrowiec-Białoń, J. (2015). Supported Zirconium-Based Continuous-Flow Microreactor for Effective Meerwein-Ponndorf-Verley

- Reduction of Cyclohexanone. *Catal. Commun.* 64, 48–51. doi:10.1016/j.catcom.2015.01.021
- Kou, H., Luo, W., Huang, Z., Sang, G., Hu, C., Chen, C., et al. (2016). Effects of Temperature and Hydrogen Pressure on the Activation Behavior of Zrco. *Int. J. Hydrogen Energ.* 41, 10811–10818. doi:10.1016/j.ijhydene.2016.05.011
- Kumar, A., Kumar, N., Baredar, P., and Shukla, A. (2015). A Review on Biomass Energy Resources, Potential, Conversion and Policy in India. *Renew. Sustain. Energy. Rev.* 45, 530–539. doi:10.1016/j.rser.2015.02.007
- Kuwahara, Y., Kaburagi, W., and Fujitani, T. (2014). Catalytic Conversion of Levulinic Acid and its Esters to γ -Valerolactone over Silica-Supported Zirconia Catalysts. *Bcsj* 87, 1252–1254. doi:10.1246/bcsj.20140205
- Kuwahara, Y., Kaburagi, W., Osada, Y., Fujitani, T., and Yamashita, H. (2017). Catalytic Transfer Hydrogenation of Biomass-Derived Levulinic Acid and its Esters to γ -valerolactone over ZrO₂ Catalyst Supported on SBA-15 Silica. *Catal. Today* 281, 418–428. doi:10.1016/j.cattod.2016.05.016
- Kuwahara, Y., Kango, H., and Yamashita, H. (2016). Catalytic Transfer Hydrogenation of Biomass-Derived Levulinic Acid and its Esters to γ -Valerolactone over Sulfonic Acid-Functionalized UiO-66. *ACS Sustain. Chem. Eng.* 5, 1141–1152. doi:10.1021/acsschemeng.6b02464
- Li, F., France, L. J., Cai, Z., Li, Y., Liu, S., Lou, H., et al. (2017). Catalytic Transfer Hydrogenation of Butyl Levulinate to γ -valerolactone over Zirconium Phosphates with Adjustable Lewis and Brønsted Acid Sites. *Appl. Catal. B: Environ.* 214, 67–77. doi:10.1016/j.apcatb.2017.05.013
- Li, H., Dai, M., Dai, S., and Dong, X. (2018a). Current Status and Environment Impact of Direct Straw Return in China's Cropland - a Review. *Ecotoxicology Environ. Saf.* 159, 293–300. doi:10.1016/j.ecoenv.2018.05.014
- Li, H., Fang, Z., Smith, R. L., and Yang, S. (2016a). Efficient Valorization of Biomass to Biofuels with Bifunctional Solid Catalytic Materials. *Prog. Energ. Combustion Sci.* 55, 98–194. doi:10.1016/j.peccs.2016.04.004
- Li, H., Fang, Z., and Yang, S. (2016a). Direct Catalytic Transformation of Biomass Derivatives into Biofuel Component γ -Valerolactone with Magnetic Nickel-Zirconium Nanoparticles. *Chempluschem* 81, 135–142. doi:10.1002/cplu.201500492
- Li, H., Fang, Z., and Yang, S. (2015). Direct Conversion of Sugars and Ethyl Levulinate into γ -Valerolactone with Superparamagnetic Acid-Base Bifunctional Zr/FeOx Nanocatalysts. *ACS Sustain. Chem. Eng.* 4, 236–246. doi:10.1021/acsschemeng.5b01480
- Li, H., Guo, H., Fang, Z., Aida, T. M., and Smith, R. L. (2020a). Cycloamination Strategies for Renewable N-Heterocycles. *Green. Chem.* 22, 582–611. doi:10.1039/c9gc03655e
- Li, H., He, J., Riisager, A., Saravanamurugan, S., Song, B., and Yang, S. (2016c). Acid-Base Bifunctional Zirconium N-Alkyltriphosphate Nanohybrid for Hydrogen Transfer of Biomass-Derived Carboxides. *ACS Catal.* 6, 7722–7727. doi:10.1021/acscatal.6b02431
- Li, H., Li, Y., Fang, Z., and Smith, R. L. (2019a). Efficient Catalytic Transfer Hydrogenation of Biomass-Based Furfural to Furfuryl Alcohol with Recyclable Hf-Phenylphosphonate Nanohybrids. *Catal. Today* 319, 84–92. doi:10.1016/j.cattod.2018.04.056
- Li, H., Wang, C., Xu, Y., Yu, Z., Saravanamurugan, S., Wu, Z., et al. (2020b). Heterogeneous (de)chlorination-enabled control of reactivity in the liquid-phase synthesis of furanic biofuel from cellulosic feedstock. *Green. Chem.* 22, 637–645. doi:10.1039/c9gc04092g
- Li, H., Wu, H., Zhang, H., Su, Y., Yang, S., and Hensen, E. J. M. (2019b). A Facile Direct Route to N-(Un)substituted Lactams by Cycloamination of Oxocarboxylic Acids without External Hydrogen. *Chemsuschem* 12, 3778–3784. doi:10.1002/cssc.201901780
- Li, H., Yang, T., and Fang, Z. (2018b). Biomass-derived Mesoporous Hf-Containing Hybrid for Efficient Meerwein-Ponndorf-Verley Reduction at Low Temperatures. *Appl. Catal. B: Environ.* 227, 79–89. doi:10.1016/j.apcatb.2018.01.017
- Li, H., Zhao, W., Dai, W., Long, J., Watanabe, M., Meier, S., et al. (2018). Noble Metal-free Upgrading of Multi-Unsaturated Biomass Derivatives at Room Temperature: Silyl Species Enable Reactivity. *Green. Chem.* 20, 5327–5335. doi:10.1039/c8gc02934b
- Li, H., Zhao, W., Saravanamurugan, S., Dai, W., He, J., Meier, S., et al. (2018). Control of Selectivity in Hydrosilane-Promoted Heterogeneous Palladium-Catalyzed Reduction of Furfural and Aromatic Carboxides. *Commun. Chem.* 1. doi:10.1038/s42004-018-0033-z
- Li, J., Zhao, S., Li, Z., Liu, D., Chi, Y., and Hu, C. (2021). Efficient Conversion of Biomass-Derived Levulinic Acid to γ -Valerolactone over Polyoxometalate@Zr-Based Metal-Organic Frameworks: The Synergistic Effect of Brønsted and Lewis Acidic Sites. *Inorg. Chem.* 60, 7785–7793. doi:10.1021/acs.inorgchem.1c00185
- Li, M., Liu, Y., Lin, X., Tan, J., Yang, S., and Li, H. (2021). One-step Upgrading of Bio-Based Furfural to γ -valerolactone via HfCl₄-Mediated Bifunctional Catalysis. *RSC Adv.* 11, 35415–35424. doi:10.1039/d1ra05637a
- Li, W., Cai, Z., Li, H., Shen, Y., Zhu, Y., Li, H., et al. (2019). Hf-based Metal Organic Frameworks as Bifunctional Catalysts for the One-Pot Conversion of Furfural to γ -valerolactone. *Mol. Catal.* 472, 17–26. doi:10.1016/j.mcat.2019.04.010
- Li, X., Du, Z., Wu, Y., Zhen, Y., Shao, R., Li, B., et al. (2020). A Novel Hafnium-Graphite Oxide Catalyst for the Meerwein-Ponndorf-Verley Reaction and the Activation Effect of the Solvent. *RSC Adv.* 10, 9985–9995. doi:10.1039/c9ra10795a
- Li, X., and Jiang, J. (2019). Molecular Design of Chiral Zirconium Metal-Organic Frameworks for Asymmetric Transfer Hydrogenation of Imines. *Catal. Sci. Technol.* 9, 4888–4897. doi:10.1039/c9cy00770a
- Liao, Y., Liu, Q., Wang, T., Long, J., Ma, L., and Zhang, Q. (2014). Zirconium Phosphate Combined with Ru/C as a Highly Efficient Catalyst for the Direct Transformation of Cellulose to C₆ Alditols. *Green. Chem.* 16, 3305–3312. doi:10.1039/c3gc42444h
- Lin, Y., Bu, Q., Xu, J., Liu, X., Zhang, X., Lu, G.-P., et al. (2021). Hf-MOF Catalyzed Meerwein-Ponndorf-Verley (MPV) Reduction Reaction: Insight into Reaction Mechanism. *Mol. Catal.* 502, 111405. doi:10.1016/j.mcat.2021.11.1405
- Liu, C., Wei, L., Yin, X., Pan, X., Hu, J., Li, N., et al. (2021). Synthesis of Furfural from Xylan in γ -valerolactone/molten Salt Hydrate Biphasic System. *Chem. Eng. J.* 425, 130608. doi:10.1016/j.cej.2021.130608
- Liu, C., Xu, G., Hu, A., Xie, Y., and Wang, H. (2019). Porous Zirconium Hydroxyphosphonoacetate: Catalyst for Conversion of Furfural into Furfuryl Alcohol. *Chemistryselect* 4, 8000–8006. doi:10.1002/slct.201901612
- Liu, K., Qin, R., and Zheng, N. (2021). Insights into the Interfacial Effects in Heterogeneous Metal Nanocatalysts toward Selective Hydrogenation. *J. Am. Chem. Soc.* 143, 4483–4499. doi:10.1021/jacs.0c13185
- Liu, S. H., Jaenicke, S., and Chuah, G. K. (2002). Hydrous Zirconia as a Selective Catalyst for the Meerwein-Ponndorf-Verley Reduction of Cinnamaldehyde. *J. Catal.* 206, 321–330. doi:10.1006/jcat.2001.3480
- Liu, S., Meng, Y., Li, H., and Yang, S. (2021). Hierarchical Porous mil-101(Cr) Solid Acid-Catalyzed Production of Value-Added Acetals from Biomass-Derived Furfural. *Polymers* 13, 3498. doi:10.3390/polym13203498
- Liu, X., Yin, B., Zhang, W., Yu, X., Du, Y., Zhao, S., et al. (2021). Catalytic Transfer Hydrogenolysis of Glycerol over Heterogeneous Catalysts: A Short Review on Mechanistic Studies. *Chem. Rec.* 21, 1792–1810. doi:10.1002/tcr.202100037
- Liu, Y., Chen, D., Li, M., Zhang, H., and Li, H. (2021). Catalytic Stereoselective Conversion of Biomass-Derived 4'-Methoxypropiophenone to Trans-anethole with a Bifunctional and Recyclable Hf-Based Polymeric Nanocatalyst. *Polymers* 13, 2808. doi:10.3390/polym13162808
- Luo, H. Y., Consoli, D. F., Gunther, W. R., and Román-Leshkov, Y. (2014). Investigation of the Reaction Kinetics of Isolated Lewis Acid Sites in Beta Zeolites for the Meerwein-Ponndorf-Verley Reduction of Methyl Levulinate to γ -valerolactone. *J. Catal.* 320, 198–207. doi:10.1016/j.jcat.2014.10.010
- Luo, Y.-J., Zhou, Y.-H., and Huang, Y.-B. (2018). A New Lewis Acidic Zr Catalyst for the Synthesis of Furanic Diesel Precursor from Biomass Derived Furfural and 2-methylfuran. *Catal. Lett.* 149, 292–302. doi:10.1007/s10562-018-2599-6
- Luo, Y., Li, Z., Li, X., Liu, X., Fan, J., Clark, J. H., et al. (2019). The Production of Furfural Directly from Hemicellulose in Lignocellulosic Biomass: A Review. *Catal. Today* 319, 14–24. doi:10.1016/j.cattod.2018.06.042
- Ma, M., Yan, X., Hou, P., Cao, J., Liu, H., Xu, X., et al. (2020). One-Pot Transfer Hydrogenation of Methyl Levulinate into Valerolactone and 1,4-pentanediol over *In Situ* Reduced Cu/ZrOCO₃ in 2-PrOH. *Chemistryselect* 5, 924–930. doi:10.1002/slct.201904480
- Mardiana, S., Azhari, N. J., Ilmi, T., and Kadja, G. T. M. (2022). Hierarchical Zeolite for Biomass Conversion to Biofuel: A Review. *Fuel* 309, 122119. doi:10.1016/j.fuel.2021.122119
- Mathimani, T., and Mallick, N. (2019). A Review on the Hydrothermal Processing of Microalgal Biomass to Bio-Oil - Knowledge Gaps and Recent Advances. *J. Clean. Prod.* 217, 69–84. doi:10.1016/j.jclepro.2019.01.129
- Mautschke, H. H., and Llabrés i Xamena, F. X. (2021). One-Step Chemo-, Regio- and Stereoselective Reduction of Ketosteroids to Hydroxysteroids over Zr-

- Containing MOF-808 Metal-Organic Frameworks. *Chem. Eur. J.* 27, 10766–10775. doi:10.1002/chem.202100967
- Melero, J. A., Morales, G., Iglesias, J., Paniagua, M., and López-Aguado, C. (2018). Rational Optimization of Reaction Conditions for the One-Pot Transformation of Furfural to γ -Valerolactone over Zr-Al-Beta Zeolite: Toward the Efficient Utilization of Biomass. *Ind. Eng. Chem. Res.* 57, 11592–11599. doi:10.1021/acs.iecr.8b02475
- Melero, J. A., Morales, G., Iglesias, J., Paniagua, M., López-Aguado, C., Wilson, K., et al. (2017). Efficient One-Pot Production of γ -valerolactone from Xylose over Zr-Al-Beta Zeolite: Rational Optimization of Catalyst Synthesis and Reaction Conditions. *Green. Chem.* 19, 5114–5121. doi:10.1039/c7gc01969f
- Mondelli, C., Gözaydın, G., Yan, N., and Pérez-Ramírez, J. (2020). Biomass Valorisation over Metal-Based Solid Catalysts from Nanoparticles to Single Atoms. *Chem. Soc. Rev.* 49, 3764–3782. doi:10.1039/d0cs00130a
- Nguyen, L. H. T., Nguyen, T. T. T., Tran, P. H., Kawazoe, Y., Le, H. M., and Doan, T. L. H. (2019). Zr and Hf-Metal-Organic Frameworks: Efficient and Recyclable Heterogeneous Catalysts for the Synthesis of 2-arylbenzoxazole via Ring Open Pathway Acylation Reaction. *J. Catal.* 374, 110–117. doi:10.1016/j.jcat.2019.04.023
- Osman, A. I., Mehta, N., Elgarahy, A. M., Al-Hinai, A., Al-Muhtaseb, A. A. H., and Rooney, D. W. (2021). Conversion of Biomass to Biofuels and Life Cycle Assessment: A Review. *Environ. Chem. Lett.* 19, 4075–4118. doi:10.1007/s10311-021-01273-0
- Palermo, V., Kinloch, I. A., Ligi, S., and Pugno, N. M. (2016). Nanoscale Mechanics of Graphene and Graphene Oxide in Composites: A Scientific and Technological Perspective. *Adv. Mater.* 28, 6232–6238. doi:10.1002/adma.201505469
- Pan, H., Xia, Q., Li, H., Wang, Y., Shen, Z., Wang, Y., et al. (2022). Direct Production of Biodiesel from Crude *euphorbia* Lathyrus L. Oil Catalyzed by Multifunctional Mesoporous Composite Materials. *Fuel* 309, 122172. doi:10.1016/j.fuel.2021.122172
- Pang, J., Sun, J., Zheng, M., Li, H., Wang, Y., and Zhang, T. (2019). Transition Metal Carbide Catalysts for Biomass Conversion: A Review. *Appl. Catal. B: Environ.* 254, 510–522. doi:10.1016/j.apcatb.2019.05.034
- Paniagua, M., Morales, G., Melero, J. A., Iglesias, J., López-Aguado, C., Vidal, N., et al. (2021). Understanding the Role of Al/Zr Ratio in Zr-Al-Beta Zeolite: Towards the One-Pot Production of Gvl from Glucose. *Catal. Today* 367, 228–238. doi:10.1016/j.cattod.2020.04.025
- Pattnaik, F., Tripathi, S., Patra, B. R., Nanda, S., Kumar, V., Dalai, A. K., et al. (2021). Catalytic Conversion of Lignocellulosic Polysaccharides to Commodity Biochemicals: A Review. *Environ. Chem. Lett.* 19, 4119–4136. doi:10.1007/s10311-021-01284-x
- Peng, Q., Wang, H., Xia, Y., and Liu, X. (2021). One-pot Conversion of Furfural to Gamma-Valerolactone in the Presence of Multifunctional Zirconium Alizarin Red S Hybrid. *Appl. Catal. A: Gen.* 621, 118203. doi:10.1016/j.apcata.2021.118203
- Prasertsab, A., Maihom, T., Probst, M., Wattanakit, C., and Limtrakul, J. (2018). Furfural to Furfuryl Alcohol: Computational Study of the Hydrogen Transfer on Lewis Acidic Bea Zeolites and Effects of Cation Exchange and Tetravalent Metal Substitution. *Inorg. Chem.* 57, 6599–6605. doi:10.1021/acs.inorgchem.8b00741
- Prasomsri, T., Nimmanwudipong, T., and Román-Leshkov, Y. (2013). Effective Hydrodeoxygenation of Biomass-Derived Oxygenates into Unsaturated Hydrocarbons by MoO₃ Using Low H₂ Pressures. *Energy Environ. Sci.* 6, 1732–1738. doi:10.1039/c3ee24360e
- Priecel, P., Endot, N. A., Carà, P. D., and Lopez-Sanchez, J. A. (2018). Fast Catalytic Hydrogenation of 2,5-hydroxymethylfurfural to 2,5-dimethylfuran with Ruthenium on Carbon Nanotubes. *Ind. Eng. Chem. Res.* 57, 1991–2002. doi:10.1021/acs.iecr.7b04715
- Ramanathan, A., Castro Villalobos, M. C., Kwakernaak, C., Telalovic, S., and Hanefeld, U. (2008). Zr-TUD-1: A Lewis Acidic, Three-Dimensional, Mesoporous, Zirconium-Containing Catalyst. *Chem. Eur. J.* 14, 961–972. doi:10.1002/chem.200700725
- Rode, A., Carleton, T., Delgado, M., Greenstone, M., Houser, T., Hsiang, S., et al. (2021). Estimating a Social Cost of Carbon for Global Energy Consumption. *Nature* 598, 308–314. doi:10.1038/s41586-021-03883-8
- Rojas-Buzo, S., García-García, P., and Corma, A. (2018). Catalytic Transfer Hydrogenation of Biomass-Derived Carbonyls over Hafnium-Based Metal-Organic Frameworks. *ChemSuschem* 11, 432–438. doi:10.1002/cssc.201701708
- Rui, T., Lu, G.-P., Zhao, X., Cao, X., and Chen, Z. (2021). The Synergistic Catalysis on Co Nanoparticles and Conx Sites of Aniline-Modified Zif Derived Co@ncs for Oxidative Esterification of HMF. *Chin. Chem. Lett.* 32, 685–690. doi:10.1016/j.ccllet.2020.06.027
- Sabyrzhan, A., Balgimbekova, G., and Shestak, V. (2021). Economic and Legal Regulation of the Use and Development of Renewable Energy Sources. *Int. Environ. Agreements* 21, 595–610. doi:10.1007/s10784-021-09532-9
- Sakakibara, K., Endo, K., and Osawa, T. (2019). Facile Synthesis of γ -valerolactone by Transfer Hydrogenation of Methyl Levulinate and Levulinic Acid over Ni/ZrO₂. *Catal. Commun.* 125, 52–55. doi:10.1016/j.catcom.2019.03.021
- Santana, C. G., and Krische, M. J. (2021). From Hydrogenation to Transfer Hydrogenation to Hydrogen Auto-Transfer in Enantioselective Metal-Catalyzed Carbonyl Reductive Coupling: Past, Present, and Future. *ACS Catal.* 11, 5572–5585. doi:10.1021/acscatal.1c01109
- Sarkar, C., Paul, R., Chandra Shit, S., Trinh, Q. T., Koley, P., Rao, B. S., et al. (2021). Navigating Copper-Atom-Pair Structural Effect inside a Porous Organic Polymer Cavity for Selective Hydrogenation of Biomass-Derived 5-hydroxymethylfurfural. *ACS Sustain. Chem. Eng.* 9, 2136–2151. doi:10.1021/acscuschemeng.0c07594
- Schwarzman, M., Schildroth, S., Bhetraratana, M., Alvarado, Á., and Balmes, J. (2021). Raising Standards to Lower Diesel Emissions. *Science* 371, 1314–1316. doi:10.1126/science.abf8159
- Sha, Y., Xiao, Z., Zhou, H., Yang, K., Song, Y., Li, N., et al. (2017). Direct Use of Humic Acid Mixtures to Construct Efficient Zr-Containing Catalysts for Meerwein-Ponndorf-Verley Reactions. *Green. Chem.* 19, 4829–4837. doi:10.1039/c7gc01925d
- Shao, Y., Li, Q., Dong, X., Wang, J., Sun, K., Zhang, L., et al. (2021). Cooperation between Hydrogenation and Acidic Sites in Cu-Based Catalyst for Selective Conversion of Furfural to γ -valerolactone. *Fuel* 293, 120457. doi:10.1016/j.fuel.2021.120457
- Shearer, G. C., Chavan, S., Ethiraj, J., Vitillo, J. G., Svelle, S., Olsbye, U., et al. (2014). Tuned to Perfection: Ironing Out the Defects in Metal-Organic Framework UiO-66. *Chem. Mater.* 26, 4068–4071. doi:10.1021/cm501859p
- Shen, S., Chen, J., Koodali, R. T., Hu, Y., Xiao, Q., Zhou, J., et al. (2014). Activation of MCM-41 Mesoporous Silica by Transition-Metal Incorporation for Photocatalytic Hydrogen Production. *Appl. Catal. B: Environ.* 150–151, 138–146. doi:10.1016/j.apcatb.2013.12.014
- Shi, D., Yang, Q., Peterson, C., Lamic-Humblot, A.-F., Girardon, J.-S., Griboval-Constant, A., et al. (2019). Bimetallic Fe-Ni/SiO₂ Catalysts for Furfural Hydrogenation: Identification of the Interplay between Fe and Ni during Deposition-Precipitation and Thermal Treatments. *Catal. Today* 334, 162–172. doi:10.1016/j.cattod.2018.11.041
- Silbernagel, R., Martin, C. H., and Clearfield, A. (2016). Zirconium(IV) Phosphonate-Phosphates as Efficient Ion-Exchange Materials. *Inorg. Chem.* 55, 1651–1656. doi:10.1021/acs.inorgchem.5b02555
- Singh, J., Suhag, M., and Dhaka, A. (2015). Augmented Digestion of Lignocellulose by Steam Explosion, Acid and Alkaline Pretreatment Methods: A Review. *Carbohydr. Polym.* 117, 624–631. doi:10.1016/j.carbpol.2014.10.012
- Solanki, B. S., and Rode, C. V. (2019). Selective Hydrogenation of 5-HMF to 2,5-DMF over a Magnetically Recoverable Non-noble Metal Catalyst. *Green. Chem.* 21, 6390–6406. doi:10.1039/c9gc03091c
- Song, J., Hua, M., Huang, X., Visa, A., Wu, T., Fan, H., et al. (2021). Highly Efficient Meerwein-Ponndorf-Verley Reductions over a Robust Zirconium-Organoboronic Acid Hybrid. *Green. Chem.* 23, 1259–1265. doi:10.1039/d0gc04179c
- Song, J., Wu, L., Zhou, B., Zhou, H., Fan, H., Yang, Y., et al. (2015). A New Porous Zr-Containing Catalyst with a Phenate Group: an Efficient Catalyst for the Catalytic Transfer Hydrogenation of Ethyl Levulinate to γ -valerolactone. *Green. Chem.* 17, 1626–1632. doi:10.1039/c4gc02104e
- Song, J., Zhou, B., Zhou, H., Wu, L., Meng, Q., Liu, Z., et al. (2015). Porous Zirconium-Phytic Acid Hybrid: A Highly Efficient Catalyst for Meerwein-Ponndorf-Verley Reductions. *Angew. Chem. Int. Ed.* 54, 9399–9403. doi:10.1002/anie.201504001
- Spinelli, R., Visser, R., Björheden, R., and Röser, D. (2019). Recovering Energy Biomass in Conventional forest Operations: A Review of Integrated Harvesting Systems. *Curr. For. Rep.* 5, 90–100. doi:10.1007/s40725-019-00089-0
- Srinivasa Rao, B., Krishna Kumari, P., Dhana Lakshmi, D., and Lingaiah, N. (2018). One Pot Selective Transformation of Biomass Derived Chemicals towards Alkyl

- Levulinates over Titanium Exchanged Heteropoly Tungstate Catalysts. *Catal. Today* 309, 269–275. doi:10.1016/j.cattod.2017.05.040
- Srinivasa Rao, B., Yogita Dhana Lakshmi, D., Dhana Lakshmi, D., Kumari, P. K., and Lingaiah, N. (2021). Influence of Metal Oxide and Heteropoly Tungstate Location in Mesoporous Silica towards Catalytic Transfer Hydrogenation of Furfural to γ -valerolactone. *Sustain. Energ. Fuels* 5, 3719–3728. doi:10.1039/d1se00340b
- Sudarsanam, P., Li, H., and Sagar, T. V. (2020). TiO₂-Based Water-Tolerant Acid Catalysis for Biomass-Based Fuels and Chemicals. *ACS Catal.* 10, 9555–9584. doi:10.1021/acscatal.0c01680
- Sullivan, M. M., Chen, C.-J., and Bhan, A. (2016). Catalytic Deoxygenation on Transition Metal Carbide Catalysts. *Catal. Sci. Technol.* 6, 602–616. doi:10.1039/c5cy01665g
- Sushkevich, V. L., Ivanova, I. I., Tolborg, S., and Taarning, E. (2014). Meerwein-Ponndorf-Verley-Oppenauer Reaction of Crotonaldehyde with Ethanol over Zr-Containing Catalysts. *J. Catal.* 316, 121–129. doi:10.1016/j.jcat.2014.04.019
- Synowiecki, J., and Al-Khateeb, N. A. (2003). Production, Properties, and Some New Applications of Chitin and its Derivatives. *Crit. Rev. Food Sci. Nutr.* 43, 145–171. doi:10.1080/10408690390826473
- Tan, J., Li, Y., Tan, X., Wu, H., Li, H., and Yang, S. (2021). Advances in Pretreatment of Straw Biomass for Sugar Production. *Front. Chem.* 9, 696030. doi:10.3389/fchem.2021.696030
- Tan, X., Zhang, H., Li, H., and Yang, S. (2022). Electrovalent Bifunctional Acid Enables Heterogeneously Catalytic Production of Biodiesel by (Trans) esterification of Non-edible Oils. *Fuel* 310, 122273. doi:10.1016/j.fuel.2021.122273
- Tang, X., Chen, H., Hu, L., Hao, W., Sun, Y., Zeng, X., et al. (2014a). Conversion of Biomass to γ -valerolactone by Catalytic Transfer Hydrogenation of Ethyl Levulinate over Metal Hydroxides. *Appl. Catal. B: Environ.* 147, 827–834. doi:10.1016/j.apcatb.2013.10.021
- Tang, X., Hu, L., Sun, Y., Zhao, G., Hao, W., and Lin, L. (2013). Conversion of Biomass-Derived Ethyl Levulinate into γ -valerolactone via Hydrogen Transfer from Supercritical Ethanol over a ZrO₂ Catalyst. *RSC Adv.* 3, 10277. doi:10.1039/c3ra41288a
- Tang, X., Zeng, X., Li, Z., Hu, L., Sun, Y., Liu, S., et al. (2014b). Production of γ -valerolactone from Lignocellulosic Biomass for Sustainable Fuels and Chemicals Supply. *Renew. Sustain. Energ. Rev.* 40, 608–620. doi:10.1016/j.rser.2014.07.209
- Tang, X., Zeng, X., Li, Z., Li, W., Jiang, Y., Hu, L., et al. (2015). *In Situ* Generated Catalyst System to Convert Biomass-Derived Levulinic Acid to γ -Valerolactone. *ChemCatChem* 7, 1372–1379. doi:10.1002/cctc.201500115
- Taniya, K., Izumi, A., Ichihashi, Y., and Nishiyama, S. (2010). Influence of Preparation Methods of Supported Zr Oxide Catalysts for Meerwein-Ponndorf-Verley Reduction of Acetophenone. *Msf* 658, 420–423. doi:10.4028/www.scientific.net/msf.658.420
- Tian, Y., Zhang, F., Wang, J., Cao, L., and Han, Q. (2021). A Review on Solid Acid Catalysis for Sustainable Production of Levulinic Acid and Levulinate Esters from Biomass Derivatives. *Bioresour. Techn.* 342, 125977. doi:10.1016/j.biortech.2021.125977
- Tripathi, M., Sahu, J. N., and Ganesan, P. (2016). Effect of Process Parameters on Production of Biochar from Biomass Waste through Pyrolysis: A Review. *Renew. Sustain. Energ. Rev.* 55, 467–481. doi:10.1016/j.rser.2015.10.122
- Tuteja, J., Nishimura, S., and Ebitani, K. (2014). Base-free Chemoselective Transfer Hydrogenation of Nitroarenes to Anilines with Formic Acid as Hydrogen Source by a Reusable Heterogeneous Pd/ZrP Catalyst. *RSC Adv.* 4, 38241–38249. doi:10.1039/c4ra06174h
- Valderrama Rios, M. L., González, A. M., Lora, E. E. S., and Almazán del Olmo, O. A. (2018). Reduction of Tar Generated during Biomass Gasification: A Review. *Biomass and Bioenergy* 108, 345–370. doi:10.1016/j.biombioe.2017.12.002
- Valekar, A. H., Cho, K.-H., Chitale, S. K., Hong, D.-Y., Cha, G.-Y., Lee, U.-H., et al. (2016). Catalytic Transfer Hydrogenation of Ethyl Levulinate to γ -valerolactone over Zirconium-Based Metal-Organic Frameworks. *Green. Chem.* 18, 4542–4552. doi:10.1039/c6gc00524a
- Valekar, A. H., Lee, M., Yoon, J. W., Kwak, J., Hong, D.-Y., Oh, K.-R., et al. (2020). Catalytic Transfer Hydrogenation of Furfural to Furfuryl Alcohol under Mild Conditions over Zr-MOFs: Exploring the Role of Metal Node Coordination and Modification. *ACS Catal.* 10, 3720–3732. doi:10.1021/acscatal.9b05085
- Wagner, M., Meyer, B., Setvin, M., Schmid, M., and Diebold, U. (2021). Direct Assessment of the Acidity of Individual Surface Hydroxyls. *Nature* 592, 722–725. doi:10.1038/s41586-021-03432-3
- Wang, A., Sudarsanam, P., Xu, Y., Zhang, H., Li, H., and Yang, S. (2020). Functionalized Magnetic Nanosized Materials for Efficient Biodiesel Synthesis via Acid-Base/enzyme Catalysis. *Green. Chem.* 22, 2977–3012. doi:10.1039/d0gc00924e
- Wang, C., Liu, X., Keser Demir, N., Chen, J. P., and Li, K. (2016). Applications of Water Stable Metal-Organic Frameworks. *Chem. Soc. Rev.* 45, 5107–5134. doi:10.1039/c6cs00362a
- Wang, F., Yuan, Z., Liu, B., Chen, S., and Zhang, Z. (2016). Catalytic Oxidation of Biomass Derived 5-hydroxymethylfurfural (HMF) over Ru III-incorporated Zirconium Phosphate Catalyst. *J. Ind. Eng. Chem.* 38, 181–185. doi:10.1016/j.jiec.2016.05.001
- Wang, J., Jaenicke, S., and Chuah, G.-K. (2014). Zirconium-Beta Zeolite as a Robust Catalyst for the Transformation of Levulinic Acid to γ -valerolactone via Meerwein-Ponndorf-Verley Reduction. *RSC Adv.* 4, 13481–13489. doi:10.1039/c4ra01120a
- Wang, T., He, J., and Zhang, Y. (2020). Production of γ -Valerolactone from One-Pot Transformation of Biomass-Derived Carbohydrates over Chitosan-Supported Ruthenium Catalyst Combined with Zeolite ZSM-5. *Eur. J. Org. Chem.* 2020, 1611–1619. doi:10.1002/ejoc.201901704
- Wang, T., Xu, H., He, J., and Zhang, Y. (2020). MPV Reduction of Ethyl Levulinate to γ -valerolactone by the Biomass-Derived Chitosan-Supported Zr Catalyst. *New J. Chem.* 44, 14686–14694. doi:10.1039/d0nj02667k
- Wang, X., Hao, J., Deng, L., Zhao, H., Liu, Q., Li, N., et al. (2020). The Construction of Novel and Efficient Hafnium Catalysts Using Naturally Existing Tannic Acid for Meerwein-Ponndorf-Verley Reduction. *RSC Adv.* 10, 6944–6952. doi:10.1039/c9ra10317a
- Wang, Y., Huang, J., Lu, S., Li, P., Xia, X., Li, C., et al. (2020). Phosphorus-modified Zirconium Metal Organic Frameworks for Catalytic Transfer Hydrogenation of Furfural. *New J. Chem.* 44, 20308–20315. doi:10.1039/d0nj04285d
- Wang, Y., Lewis, J. D., and Román-Leshkov, Y. (2016). Synthesis of Itaconic Acid Ester Analogues via Self-Aldol Condensation of Ethyl Pyruvate Catalyzed by Hafnium Be Zeolites. *ACS Catal.* 6, 2739–2744. doi:10.1021/acscatal.6b00561
- Wang, Y., Tong, X., Yan, Y., Xue, S., and Zhang, Y. (2014). Efficient and Selective Conversion of Hexose to 5-hydroxymethylfurfural with Tin-Zirconium-Containing Heterogeneous Catalysts. *Catal. Commun.* 50, 38–43. doi:10.1016/j.catcom.2014.02.023
- Wei, J., Jiang, L., Huang, M., Wu, Y., and Chen, S. (2021). Intrinsic Defect Limit to the Growth of Orthorhombic HfO₂ and (Hf,Zr)O₂ with Strong Ferroelectricity: First-Principles Insights. *Adv. Funct. Mater.* 31, 2104913. doi:10.1002/adfm.202104913
- Welch, A. J., Digdya, I. A., Kent, R., Ghougassian, P., Atwater, H. A., and Xiang, C. (2021). Comparative Technoeconomic Analysis of Renewable Generation of Methane Using Sunlight, Water, and Carbon Dioxide. *ACS Energ. Lett.* 6, 1540–1549. doi:10.1021/acsenerylett.1c00174
- Winoto, H. P., Fikri, Z. A., Ha, J.-M., Park, Y.-K., Lee, H., Suh, D. J., et al. (2019). Heteropolyacid Supported on Zr-Beta Zeolite as an Active Catalyst for One-Pot Transformation of Furfural to γ -valerolactone. *Appl. Catal. B: Environ.* 241, 588–597. doi:10.1016/j.apcatb.2018.09.031
- Wu, H., Dai, W., Saravanamurugan, S., Li, H., and Yang, S. (2020). Endogenous X-C O Species Enable Catalyst-free Formylation Prerequisite for CO₂ Reductive Upgrading. *Green. Chem.* 22, 5822–5832. doi:10.1039/d0gc02142c
- Wu, H., Liu, Y., Li, H., and Yang, S. (2018). Rapid and Efficient Conversion of Bio-Based Sugar to 5-hydroxymethylfurfural Using Amino-Acid Derived Catalysts. *Energy Sour. A: Recovery, Utilization, Environ. Effects* 40, 2632–2639. doi:10.1080/15567036.2018.1505982
- Wu, H., Zhang, L.-L., Wang, J., Jiang, Y., Li, H., Sudarsanam, P., et al. (2021). Room-temperature Quasi-Catalytic Hydrogen Generation from Waste and Water. *Green. Chem.* 23, 7528–7533. doi:10.1039/d1gc02722k
- Wu, W., Li, Y., Li, H., Zhao, W., and Yang, S. (2018). Acid-Base Bifunctional Hf Nanohybrids Enable High Selectivity in the Catalytic Conversion of Ethyl Levulinate to γ -Valerolactone. *Catalysts* 8, 264. doi:10.3390/catal8070264
- Xiao, Z., Zhou, H., Hao, J., Hong, H., Song, Y., He, R., et al. (2017). A Novel and Highly Efficient Zr-Containing Catalyst Based on Humic Acids for the Conversion of Biomass-Derived Ethyl Levulinate into Gamma-Valerolactone. *Fuel* 193, 322–330. doi:10.1016/j.fuel.2016.12.072

- Xie, C., Song, J., Zhou, B., Hu, J., Zhang, Z., Zhang, P., et al. (2016). Porous Hafnium Phosphonate: Novel Heterogeneous Catalyst for Conversion of Levulinic Acid and Esters into γ -Valerolactone. *ACS Sustain. Chem. Eng.* 4, 6231–6236. doi:10.1021/acssuschemeng.6b02230
- Xie, Y., Li, F., Wang, J., Wang, R., Wang, H., Liu, X., et al. (2017). Catalytic Transfer Hydrogenation of Ethyl Levulinate to γ -valerolactone over a Novel Porous Zirconium Trimetaphosphate. *Mol. Catal.* 442, 107–114. doi:10.1016/j.mcat.2017.09.011
- Xue, Z., Jiang, J., Li, G., Zhao, W., Wang, J., and Mu, T. (2016). Zirconium-cyanuric Acid Coordination Polymer: Highly Efficient Catalyst for Conversion of Levulinic Acid to γ -valerolactone. *Catal. Sci. Technol.* 6, 5374–5379. doi:10.1039/c5cy02215k
- Yang, T., Li, H., He, J., Liu, Y., Zhao, W., Wang, Z., et al. (2017). Porous Ti/Zr Microspheres for Efficient Transfer Hydrogenation of Biobased Ethyl Levulinate to γ -Valerolactone. *ACS Omega* 2, 1047–1054. doi:10.1021/acsomega.6b00469
- Yang, Y., Liu, Q., Li, D., Tan, J., Zhang, Q., Wang, C., et al. (2017). Selective Hydrodeoxygenation of 5-hydroxymethylfurfural to 2,5-dimethylfuran on Ru-MoOx/C Catalysts. *RSC Adv.* 7, 16311–16318. doi:10.1039/c7ra00605e
- Ye, L., Han, Y., Feng, J., and Lu, X. (2020). A Review about Gvl Production from Lignocellulose: Focusing on the Full Components Utilization. *Ind. Crops Prod.* 144, 112031. doi:10.1016/j.indcrop.2019.112031
- Yin, K., and Shen, Y. (2020). Theoretical Insights into CO₂ Hydrogenation to HCOOH over Fe_xZr_{1-x}O₂ Solid Solution Catalyst. *Appl. Surf. Sci.* 528, 146926. doi:10.1016/j.apsusc.2020.146926
- Yu, Z., Li, Z., Zhang, L., Zhu, K., Wu, H., Li, H., et al. (2021). A Substituent- and Temperature-Controllable NHC-Derived Zwitterionic Catalyst Enables CO₂ Upgrading for High-Efficiency Construction of Formamides and Benzimidazoles. *Green. Chem.* 23, 5759–5765. doi:10.1039/d1gc01897c
- Yun, W.-C., Yang, M.-T., and Lin, K.-Y. A. (2019). Water-born Zirconium-Based Metal Organic Frameworks as green and Effective Catalysts for Catalytic Transfer Hydrogenation of Levulinic Acid to γ -valerolactone: Critical Roles of Modulators. *J. Colloid Interf. Sci.* 543, 52–63. doi:10.1016/j.jcis.2019.02.036
- Zantye, M. S., Arora, A., and Hasan, M. M. F. (2021). Renewable-integrated Flexible Carbon Capture: A Synergistic Path Forward to Clean Energy Future. *Energ. Environ. Sci.* 14, 3986–4008. doi:10.1039/d0ee03946b
- Zhang, B., Hao, J., Sha, Y., Zhou, H., Yang, K., Song, Y., et al. (2018). Utilization of lignite Derivatives to Construct Zr-Based Catalysts for the Conversion of Biomass-Derived Ethyl Levulinate. *Fuel* 217, 122–130. doi:10.1016/j.fuel.2017.12.064
- Zhang, H., Li, H., Wang, A., Xu, C., and Yang, S. (2020). Progress of Catalytic Valorization of Bio-Glycerol with Urea into Glycerol Carbonate as a Monomer for Polymeric Materials. *Adv. Polym. Techn.* 2020, 1, 17. doi:10.1155/2020/7207068
- Zhang, H., Nai, J., Yu, L., and Lou, X. W. (2017). Metal-organic-framework-based Materials as Platforms for Renewable Energy and Environmental Applications. *Joule* 1, 77–107. doi:10.1016/j.joule.2017.08.008
- Zhang, H., Yang, W., Roslan, I. I., Jaenicke, S., and Chuah, G.-K. (2019). A Combo Zr-HY and Al-HY Zeolite Catalysts for the One-Pot cascade Transformation of Biomass-Derived Furfural to γ -valerolactone. *J. Catal.* 375, 56–67. doi:10.1016/j.jcat.2019.05.020
- Zhang, H., Zhang, L.-L., Tan, X., Li, H., and Yang, S. (2021). Catalytic High-Yield Biodiesel Production from Fatty Acids and Non-food Oils over a Magnetically Separable Acid Nanosphere. *Ind. Crops Prod.* 173, 114126. doi:10.1016/j.indcrop.2021.114126
- Zhang, S., Liu, Y., Yang, S., and Li, H. (2021). Catalytic Upgrading of Bio-Based 5-Hydroxymethylfurfural to 2,5-Dimethylfuran with Non-Noble Metals. *Energy Technol.* 9, 2100653. doi:10.1002/ente.202100653
- Zhang, X., Han, M., Liu, G., Wang, G., Zhang, Y., Zhang, H., et al. (2019). Simultaneously High-Rate Furfural Hydrogenation and Oxidation Upgrading on Nanostructured Transition Metal Phosphides through Electrocatalytic Conversion at Ambient Conditions. *Appl. Catal. B: Environ.* 244, 899–908. doi:10.1016/j.apcatb.2018.12.025
- Zhou, P., and Zhang, Z. (2016). One-pot Catalytic Conversion of Carbohydrates into Furfural and 5-hydroxymethylfurfural. *Catal. Sci. Technol.* 6, 3694–3712. doi:10.1039/c6cy00384b
- Zhou, S., Dai, F., Chen, Y., Dang, C., Zhang, C., Liu, D., et al. (2019). Sustainable Hydrothermal Self-Assembly of Hafnium-Lignosulfonate Nanohybrids for Highly Efficient Reductive Upgrading of 5-hydroxymethylfurfural. *Green. Chem.* 21, 1421–1431. doi:10.1039/c8gc03710h
- Zhou, S., Dai, F., Xiang, Z., Song, T., Liu, D., Lu, F., et al. (2019). Zirconium-lignosulfonate Polyphenolic Polymer for Highly Efficient Hydrogen Transfer of Biomass-Derived Oxygenates under Mild Conditions. *Appl. Catal. B: Environ.* 248, 31–43. doi:10.1016/j.apcatb.2019.02.011
- Zhu, Y., Li, Z., and Chen, J. (2019). Applications of Lignin-Derived Catalysts for green Synthesis. *Green. Energ. Environ.* 4, 210–244. doi:10.1016/j.gee.2019.01.003
- Zhu, Y., Liu, S., Jaenicke, S., and Chuah, G. (2004). Zirconia Catalysts in Meerwein-Ponndorf-Verley Reduction of Citral. *Catal. Today* 97, 249–255. doi:10.1016/j.cattod.2004.07.002

Conflict of Interest: The authors declare that the research was conducted in the absence of any commercial or financial relationships that could be construed as a potential conflict of interest.

Publisher's Note: All claims expressed in this article are solely those of the authors and do not necessarily represent those of their affiliated organizations, or those of the publisher, the editors and the reviewers. Any product that may be evaluated in this article, or claim that may be made by its manufacturer, is not guaranteed or endorsed by the publisher.

Copyright © 2021 Liu, Liu, Li, Meng, Li, Zhang and Zhang. This is an open-access article distributed under the terms of the Creative Commons Attribution License (CC BY). The use, distribution or reproduction in other forums is permitted, provided the original author(s) and the copyright owner(s) are credited and that the original publication in this journal is cited, in accordance with accepted academic practice. No use, distribution or reproduction is permitted which does not comply with these terms.